Pulsar Timing Array

Atsushi Nishizawa
(Hiroshima U.)

Mar 2-5, 2026 @ KEK
Frontiers of Cosmology: From the Early Universe to Observational Tensions
(KEK Cosmo 2025)

Table of contents

Part 1:
Pulsar timing array and GW search

1. Pulsar timing array

Pulsars

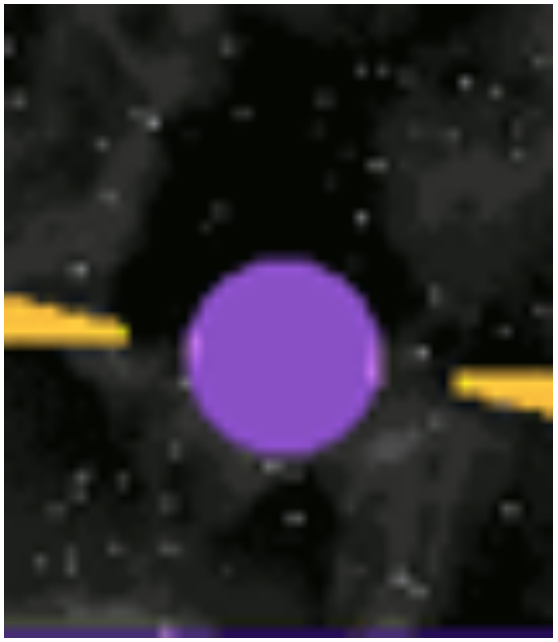

By Michael Kramer

- Neutron star is a very compact star supported by degeneracy pressure of neutrons against gravity.
- Pulsar is a rapidly rotating neutron star emitting mainly radio beams.
- The rotation axis and magnetic dipole axis do not coincide.
  ⟶ The beams are observed as pulses.

Pulse period

Bhattacharyya,
arXiv:2104.02294 (2021)

millisecond pulsar (MSP)

- very short period
  (P < 30 msec)
- extremely stable
- old age
- weak magnetic fields

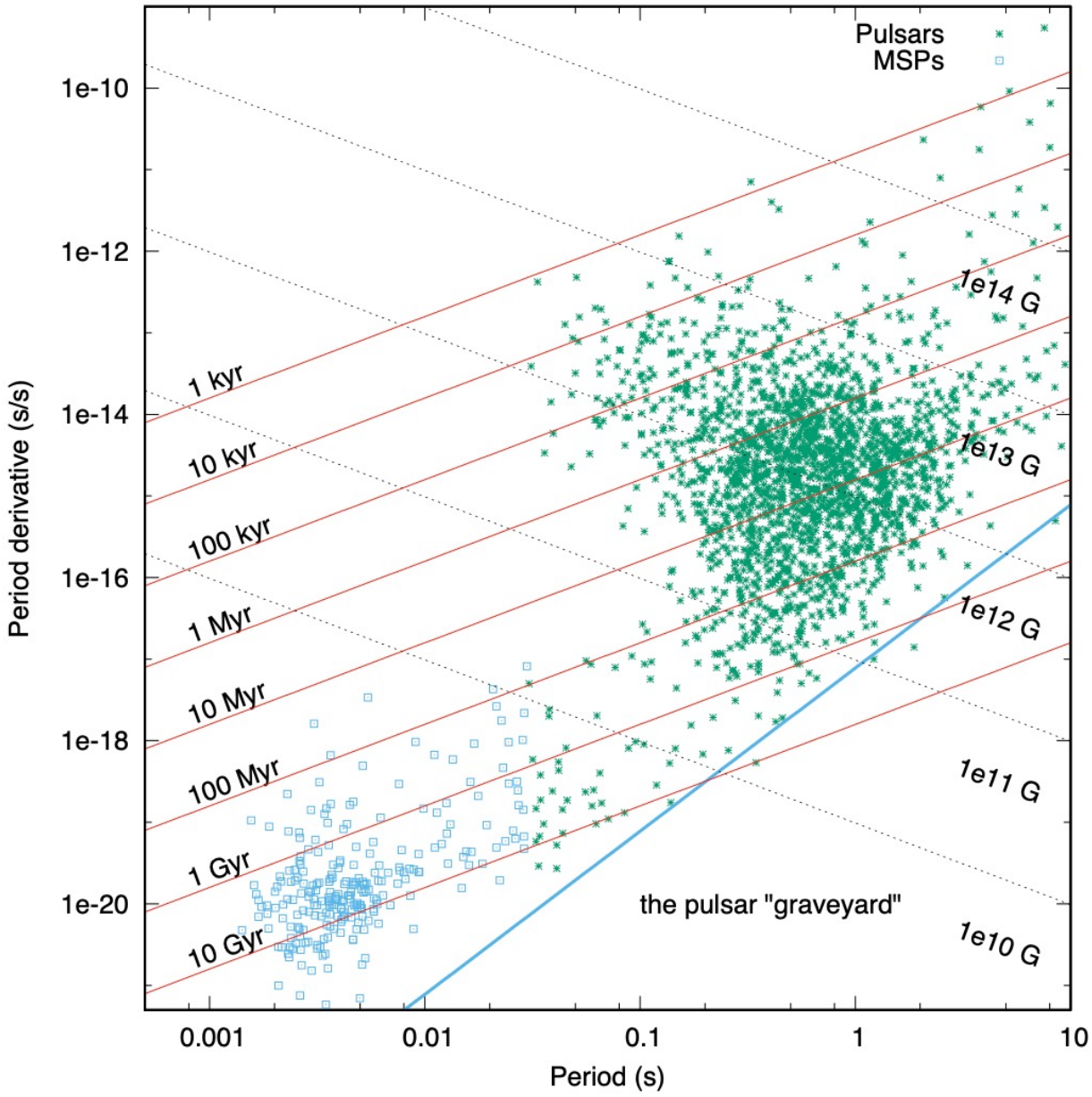

Number of pulsars discovered

Shaifullah, CQG (2025)

512 millisecond pulsars found as of 2021
(2450 ordinary pulsars)

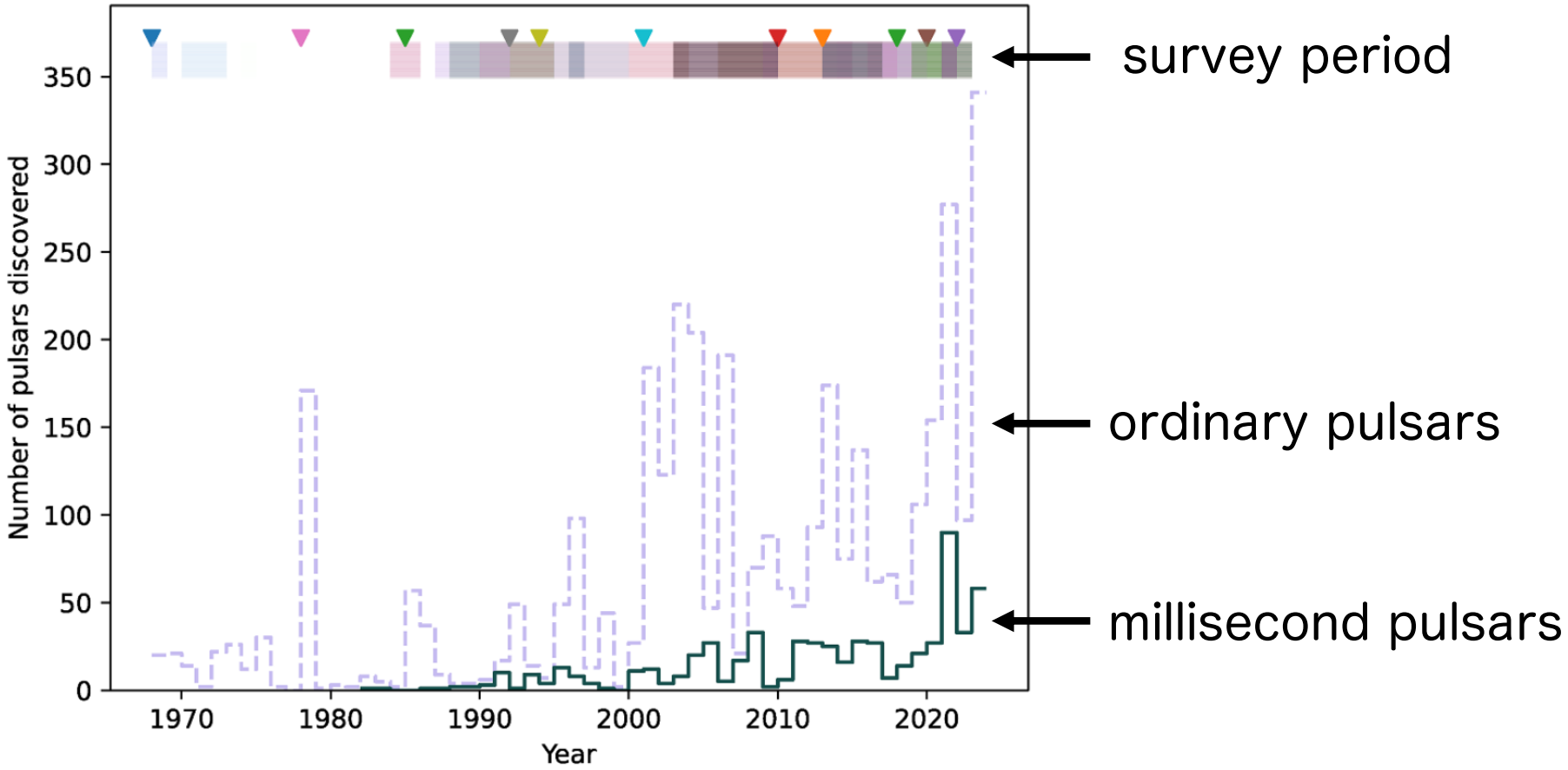

Pulse profile

Shaifullah, CQG (2025)

PSR J1713+0747

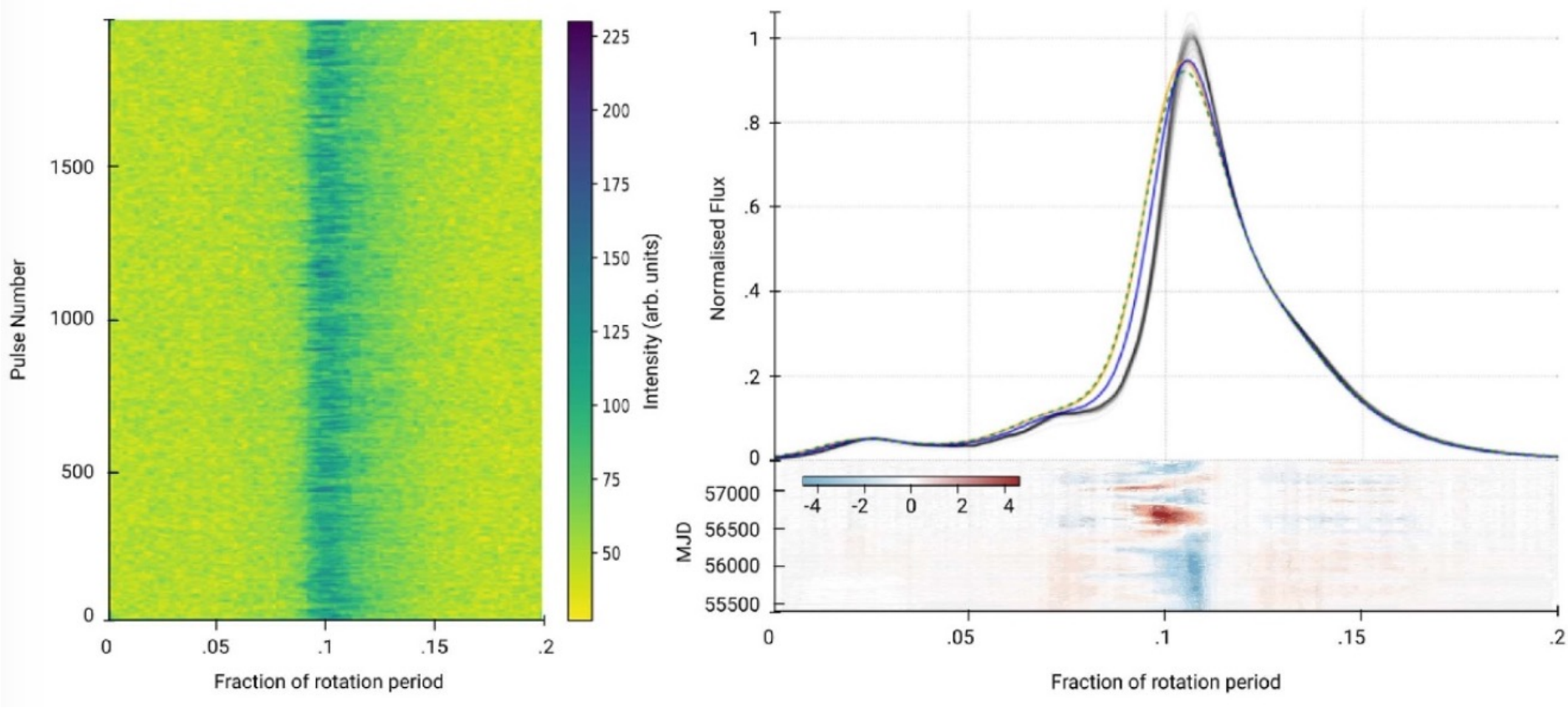

Intensity peak is stable within $\pm 1 \times 10^{-6}$ (45 nsec)

Gravitational wave observation

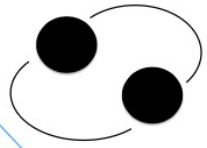

supermassive black-hole binary
(extragalactic)

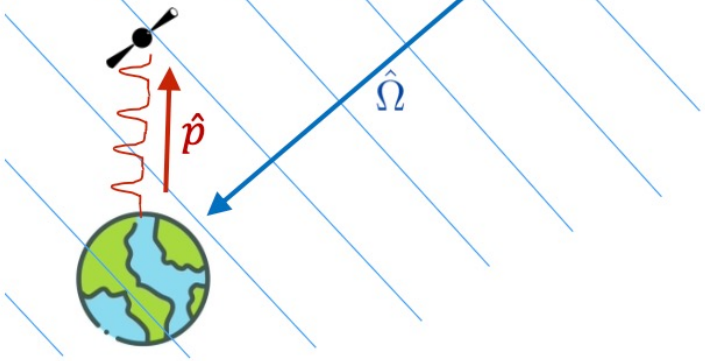

Taylor, arXiv:2511.08966 (2025)

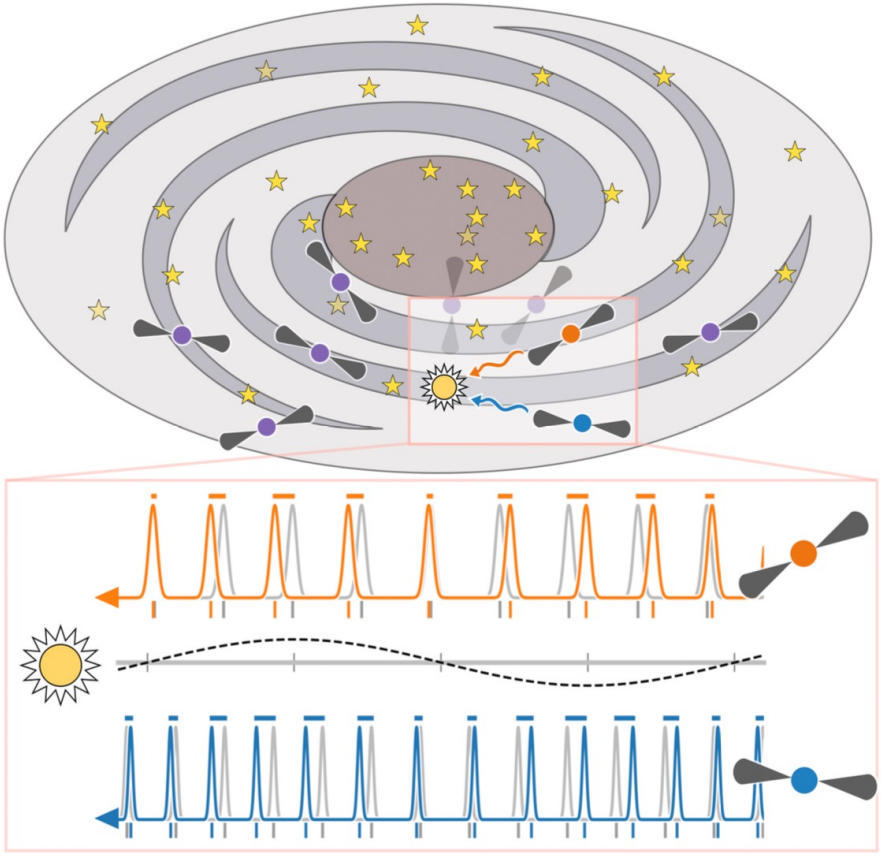

Kelley, arXiv:2505.00797 (2025)

sensitivity to GW amplitude

$$h \sim \frac{\sigma_t}{T_{\rm obs}} \sim \frac{100\,{\rm nsec}}{10\,{\rm yr}} \approx 3 \times 10^{-16}$$

GW frequency

$$f_{\rm GW} = T_{\rm obs}^{-1} \approx 3\,{\rm nHz}$$

International Pulsar Timing Array (IPTA)

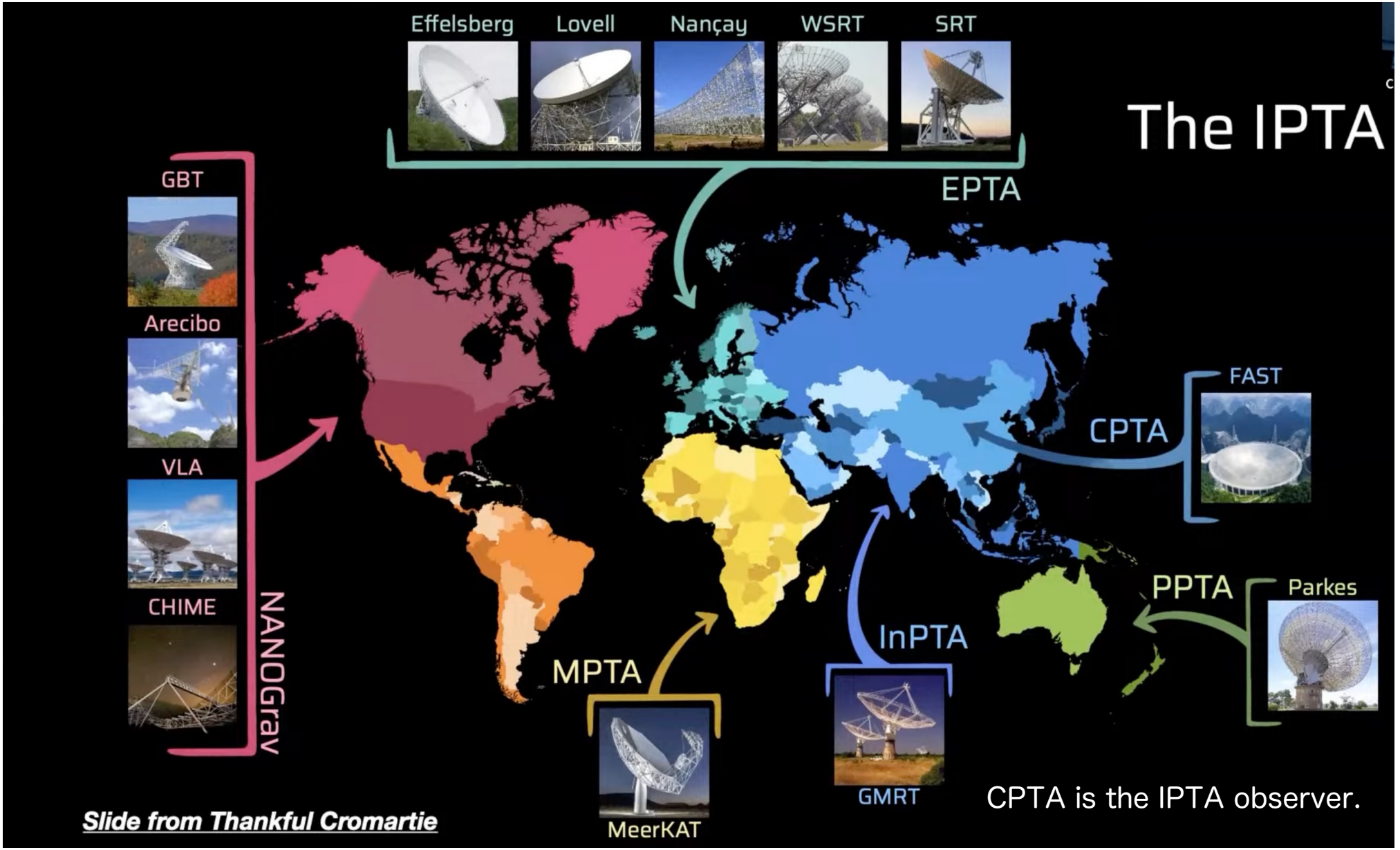

Production of time residuals

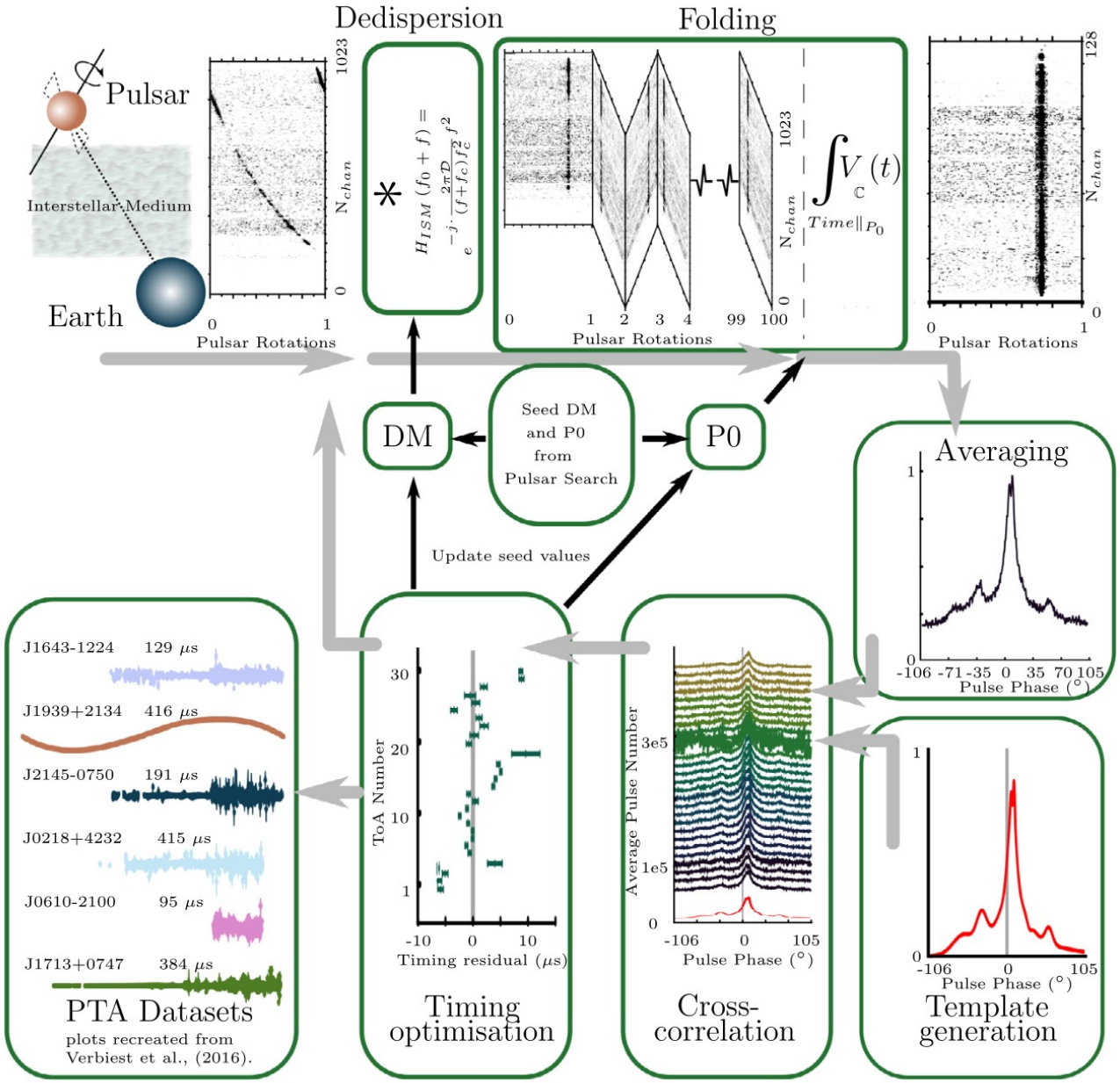

Verbiest, CQG (2018)

1. Dedispersion
2. Folding & generating average profile
3. Computing time residuals
4. Subtracting time residuals predicted by a timing model
5. Repeating the procedure and minimizing the time residuals

Timing model

arrival time $$t_{\rm a} = t_{\rm e} + \frac{d_{\odot {\rm B}}}{c} - \Delta_{\odot} - \Delta_{\rm DM} - \Delta_{\rm B}$$

$\Delta_{\odot}$: timing correction from the Solar-system barycenter

Einstein time delay (time dilation & gravitational redshift),
Shapiro time delay, Roemer time delay,
Earth atmosphere, solar wind

$\Delta_{\rm DM}$: timing correction from interstellar medium

the time variation of dispersion measure

$\Delta_{\rm B}$: timing correction from the binary barycenter (if necessary)

Einstein, Shapiro, Roemer time delays

Time residuals

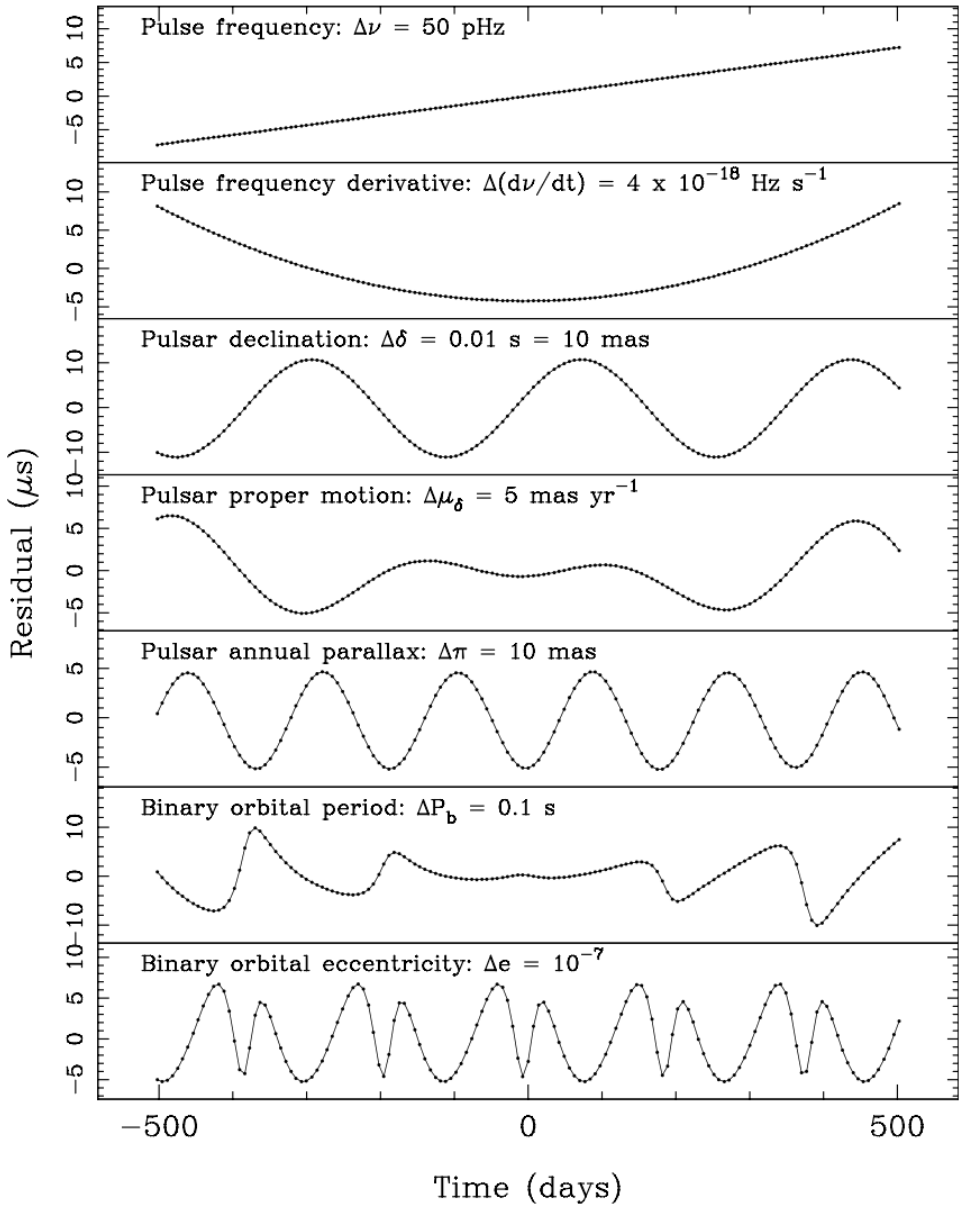

Manchester, IJMPD (2015)

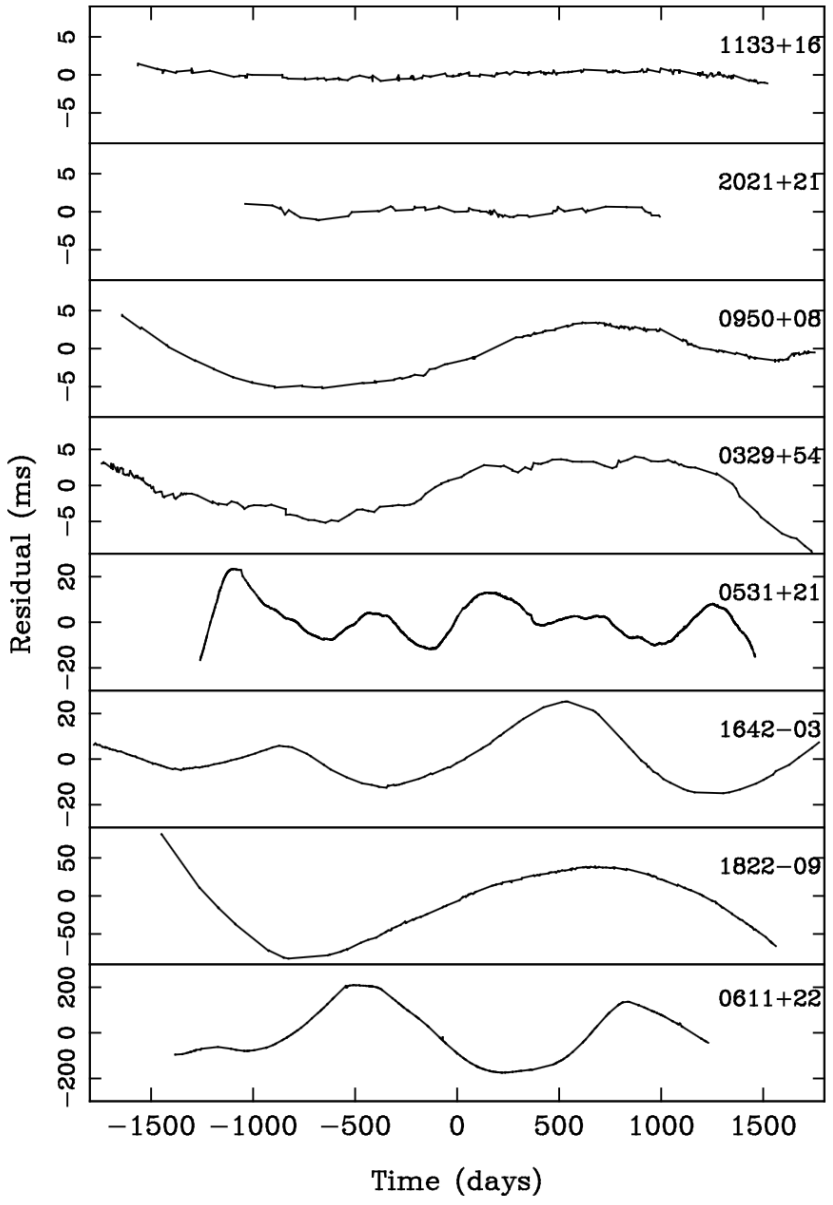

Lorimer, LRR (2008)

Noise models for time residuals

- pulsar specific red noise
  different noise spectrum for each pulsar
- common uncorrelated red noise (CURN)
  same noise spectrum for all pulsars but no phase correlation
- common monopole noise (clock error)
- common dipole noise (Solar-system ephemeris error)

common quadrupole = GW background

Correlation among multiple pulsars is necessary.

2. Principle of GW detection

Response to GW from a point source

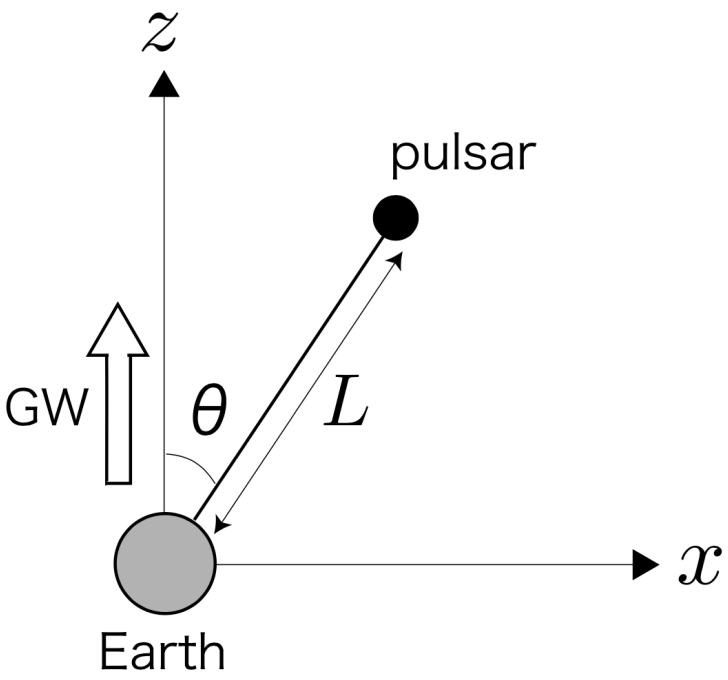

$$\mathrm{d}s^2 = -c^2\mathrm{d}t^2 + \{1 + h_+(t-z)\}\mathrm{d}x^2 + \mathrm{d}z^2$$

$$h_+(t-z) = h_+ \cos[\omega(t-z)]$$

For light ($\mathrm{d}s^2 = 0$),

$$c\,\mathrm{d}t = \left(1 + \frac{h(t-z)}{2}\sin^2\theta\right)\mathrm{d}r$$

Integrating from emission at t_1 to arrival at t_0,

$$\begin{aligned} c(t_0 - t_1) &= L - \frac{1}{2}\sin^2\theta \int_L^0 h\left[t_1 + \frac{L-r}{c} - \frac{r}{c}\cos\theta\right]\mathrm{d}r \\ &= L + \frac{1}{2}\sin^2\theta \int_0^L h\left[t_1 + \frac{L}{c} - \frac{r}{c}(1+\cos\theta)\right]\mathrm{d}r \end{aligned}$$

Response to GW from a point source

Defining $r' \equiv r(1+\cos\theta)$,

$$c(t_0 - t_1) = L + \frac{1}{2}(1-\cos\theta)\int_0^{L(1+\cos\theta)} h\left[t_1 + \frac{L}{c} - \frac{r'}{c}\right] \mathrm{d}r'$$

$$= L - \frac{c}{2}(1-\cos\theta)\left\{H\left[t_1 - \frac{L}{c}\cos\theta\right] - H\left[t_1 + \frac{L}{c}\right]\right\}$$

$$H[t] \equiv \int^t h(t')\mathrm{d}t'$$

Earth term pulsar term

$$z(t) \equiv \frac{\Delta\nu(t_0)}{\nu(t_0)} = \frac{\mathrm{d}}{\mathrm{d}t_0}(t_0 - t_1) \approx \frac{1}{2}(1-\cos\theta)\left\{h\left[t_0\right] - h\left[t_0 - \frac{L}{c}\,(1+\cos\theta)\right]\right\}$$

For a general GW propagating in the direction $\hat{\mathbf{n}}$,

$$h\sin^2\theta \to \hat{p}^i\hat{p}^j h_{ij} \ , \quad \cos\theta \to \hat{\mathbf{n}}\cdot\hat{\mathbf{p}} \qquad\qquad \tau \equiv L/c$$

$$z(t_0,\hat{\mathbf{n}}) \equiv \frac{\Delta\nu(t_0,\hat{\mathbf{n}})}{\nu(t_0)} \approx \frac{\hat{p}^i\hat{p}^j}{2(1+\hat{\mathbf{n}}\cdot\hat{\mathbf{p}})}\left\{h_{ij}\left[t_0,\hat{\mathbf{n}}\right] - h_{ij}\left[t_0 - \tau(1+\hat{\mathbf{n}}\cdot\hat{\mathbf{p}}),\hat{\mathbf{n}}\right]\right\}$$

GW response in the Fourier domain

$$z(t,\hat{\mathbf{n}}) \equiv \int_{-\infty}^{\infty} \mathrm{d}f\, \tilde{z}(f,\hat{\mathbf{n}}) e^{-2\pi i f t}$$

$$\tilde{z}(f,\hat{\mathbf{n}}) = \frac{\hat{p}^i \hat{p}^j}{2(1+\hat{\mathbf{n}}\cdot\hat{\mathbf{p}})} \tilde{h}_{ij}(f,\hat{\mathbf{n}}) \left\{1 - e^{2\pi i f \tau (1+\hat{\mathbf{n}}\cdot\hat{\mathbf{p}})}\right\}$$

Defining antenna pattern functions,

$$F^{+}(\hat{\mathbf{n}}) \equiv \frac{1}{2} \frac{\hat{p}^i \hat{p}^j}{1+\hat{\mathbf{n}}\cdot\hat{p}}\, e^{+}_{ij}(\hat{\mathbf{n}}) \;, \qquad F^{\times}(\hat{\mathbf{n}}) \equiv \frac{1}{2} \frac{\hat{p}^i \hat{p}^j}{1+\hat{\mathbf{n}}\cdot\hat{p}}\, e^{\times}_{ij}(\hat{\mathbf{n}})$$

$$\tilde{z}(f,\hat{\mathbf{n}}) = \left\{1 - e^{2\pi i f \tau (1+\hat{\mathbf{n}}\cdot\hat{\mathbf{p}})}\right\} \left\{F_{+}(\hat{\mathbf{n}}) \tilde{h}^{+}(f,\hat{\mathbf{n}}) + F_{\times}(\hat{\mathbf{n}}) \tilde{h}^{\times}(f,\hat{\mathbf{n}})\right\}$$

Cross-correlation

$$s_a(t,\hat{\mathbf{n}}) = z_a(t,\hat{\mathbf{n}}) + n_a(t)$$

correlation signal $\quad Z_{ab}(t,\hat{\mathbf{n}}) \equiv \langle s_a(t,\hat{\mathbf{n}}) s_b(t,\hat{\mathbf{n}}) \rangle$

$$\begin{aligned} Z_{ab}(t,\hat{\mathbf{n}}) &= \int_{-\infty}^{\infty} \mathrm{d}f \int_{-\infty}^{\infty} \mathrm{d}f'\, e^{2\pi i (f-f')t} \langle \tilde{s}_a^*(f,\hat{\mathbf{n}}) \tilde{s}_b(f',\hat{\mathbf{n}}) \rangle \\ &= \int_{-\infty}^{\infty} \mathrm{d}f \int_{-\infty}^{\infty} \mathrm{d}f'\, e^{2\pi i (f-f')t} \langle \tilde{z}_a^*(f,\hat{\mathbf{n}}) \tilde{z}_b(f',\hat{\mathbf{n}}) \rangle \\ &= \int_{-\infty}^{\infty} \mathrm{d}f \int_{-\infty}^{\infty} \mathrm{d}f'\, e^{2\pi i (f-f')t} \kappa_{ab}(f,f',\hat{\mathbf{n}}) \sum_A \sum_{A'} \left\langle h_A^*(f,\hat{\mathbf{n}}) h_{A'}(f',\hat{\mathbf{n}}) \right\rangle F_a^A(\hat{\mathbf{n}}) F_b^{A'}(\hat{\mathbf{n}}) \end{aligned}$$

$$\kappa_{ab}(f,f',\hat{\mathbf{n}}) \equiv \left\{ 1 - \mathrm{e}^{-2\pi i f \tau_a (1+\hat{\mathbf{n}}\cdot\hat{p}_a)} \right\} \left\{ 1 - \mathrm{e}^{2\pi i f' \tau_b (1+\hat{\mathbf{n}}\cdot\hat{p}_b)} \right\}$$

Earth term　　pulsar term

Since $f\tau_a \gg 1$, the phase factor is approximated to $\kappa_{ab} \approx 1$.
(For L=1kpc, $\tau \approx 3000\,\mathrm{yr}$)

For a GW background

A GW background is assumed to be stationary and Gaussian.

$$\langle \tilde{h}^*_A(f,\hat{\mathbf{n}})\tilde{h}_{A'}(f',\hat{\mathbf{n}}')\rangle \equiv \delta(f-f')\frac{1}{4\pi}\delta^2(\hat{\mathbf{n}},\hat{\mathbf{n}}')\frac{1}{2}S_h^{AA'}(f,\hat{\mathbf{n}})$$

In contrast to a primordial GWB, an astrophysical GWB is NOT isotropic and unpolarized.

Finite number of sources can generate a circular GWB.

Valbusa Dall'Armi+, PRL (2023); Ellis+, A&A (2023)

$$S_h^{AA'}(f,\hat{\mathbf{n}}) = \begin{pmatrix} I(f,\hat{\mathbf{n}})+Q(f,\hat{\mathbf{n}}) & U(f,\hat{\mathbf{n}})+iV(f,\hat{\mathbf{n}}) \\ U(f,\hat{\mathbf{n}})-iV(f,\hat{\mathbf{n}}) & I(f,\hat{\mathbf{n}})-Q(f,\hat{\mathbf{n}}) \end{pmatrix}$$

I : intensity, V : circular polarization

Q, U : linear polarizations (not considered hereafter)

Stokes parameters

In circular-polarization bases,

$$h_R = \frac{h_+ - ih_\times}{\sqrt{2}}, \quad h_L = \frac{h_+ + ih_\times}{\sqrt{2}}$$

$$I = |h_R|^2 + |h_L|^2, \quad \longleftarrow \text{ intensity component}$$

$$\left.\begin{aligned} Q &= h_L^* h_R + h_R^* h_L, \\ U &= i(h_L^* h_R - h_R^* h_L), \end{aligned}\right\} \text{ linear pol. components}$$

$$V = |h_R|^2 - |h_L|^2. \quad \longleftarrow \text{ circular pol. component}$$

Response to stochastic GWB

$$Z_{ab}(t) = \int_{S^2} \mathrm{d}^2\hat{\mathbf{n}}\, Z_{ab}(t,\hat{\mathbf{n}})$$

$$= \frac{1}{8\pi}\int_{-\infty}^{\infty} \mathrm{d}f \int_{S^2} \mathrm{d}^2\hat{\mathbf{n}}\, \kappa_{ab}(f,\hat{\mathbf{n}})$$

$$\times \left[I(f,\hat{\mathbf{n}}) \left\{ F_a^+(\hat{\mathbf{n}}) F_b^+(\hat{\mathbf{n}}) + F_a^\times(\hat{\mathbf{n}}) F_b^\times(\hat{\mathbf{n}}) \right\} + iV(f,\hat{\mathbf{n}}) \left\{ F_a^+(\hat{\mathbf{n}}) F_b^\times(\hat{\mathbf{n}}) - F_a^\times(\hat{\mathbf{n}}) F_b^+(\hat{\mathbf{n}}) \right\} \right]$$

$$I(f,\hat{\mathbf{n}}) = I(f) \sum_{\ell=0}^{\infty} \sum_{m=-\ell}^{\ell} c^I_{\ell m} Y_{\ell m}(\hat{\mathbf{n}}) \,, \qquad V(f,\hat{\mathbf{n}}) = V(f) \sum_{\ell=0}^{\infty} \sum_{m=-\ell}^{\ell} c^V_{\ell m} Y_{\ell m}(\hat{\mathbf{n}})$$

$$Z_{ab}(t) = \frac{1}{6\sqrt{\pi}} \int_{-\infty}^{\infty} \mathrm{d}f \left[I(f) \sum_{\ell m} c^I_{\ell m} \Gamma^I_{\ell m}(\xi_{ab}, f) + V(f) \sum_{\ell m} c^V_{\ell m} \Gamma^V_{\ell m}(\xi_{ab}, f) \right]$$

$$\Gamma^I_{\ell m}(\xi_{ab}, f) \equiv \frac{3}{4\sqrt{\pi}} \int_{S^2} \mathrm{d}^2\hat{\mathbf{n}}\, \kappa_{ab}(f,\hat{\mathbf{n}}) Y_{\ell m}(\hat{\mathbf{n}}) \left\{ F_a^+(\hat{\mathbf{n}}) F_b^+(\hat{\mathbf{n}}) + F_a^\times(\hat{\mathbf{n}}) F_b^\times(\hat{\mathbf{n}}) \right\}$$

$$\Gamma^V_{\ell m}(\xi_{ab}, f) \equiv \frac{3i}{4\sqrt{\pi}} \int_{S^2} \mathrm{d}^2\hat{\mathbf{n}}\, \kappa_{ab}(f,\hat{\mathbf{n}}) Y_{\ell m}(\hat{\mathbf{n}}) \left\{ F_a^+(\hat{\mathbf{n}}) F_b^\times(\hat{\mathbf{n}}) - F_a^\times(\hat{\mathbf{n}}) F_b^+(\hat{\mathbf{n}}) \right\}$$

Response to stochastic GWB

$$Z_{ab}(t) = \int_{S^2} \mathrm{d}^2\hat{\mathbf{n}}\, Z_{ab}(t,\hat{\mathbf{n}})$$

$$= \frac{1}{8\pi}\int_{-\infty}^{\infty} \mathrm{d}f \int_{S^2} \mathrm{d}^2\hat{\mathbf{n}}\, \kappa_{ab}(f,\hat{\mathbf{n}})$$

$$\times \left[I(f,\hat{\mathbf{n}}) \left\{ F_a^+(\hat{\mathbf{n}}) F_b^+(\hat{\mathbf{n}}) + F_a^\times(\hat{\mathbf{n}}) F_b^\times(\hat{\mathbf{n}}) \right\} + iV(f,\hat{\mathbf{n}}) \left\{ F_a^+(\hat{\mathbf{n}}) F_b^\times(\hat{\mathbf{n}}) - F_a^\times(\hat{\mathbf{n}}) F_b^+(\hat{\mathbf{n}}) \right\} \right]$$

$$I(f,\hat{\mathbf{n}}) = I(f) \sum_{\ell=0}^{\infty} \sum_{m=-\ell}^{\ell} c^I_{\ell m} Y_{\ell m}(\hat{\mathbf{n}}) \,, \qquad V(f,\hat{\mathbf{n}}) = V(f) \sum_{\ell=0}^{\infty} \sum_{m=-\ell}^{\ell} c^V_{\ell m} Y_{\ell m}(\hat{\mathbf{n}})$$

$$Z_{ab}(t) = \frac{1}{6\sqrt{\pi}} \int_{-\infty}^{\infty} \mathrm{d}f \left[I(f) \sum_{\ell m} c^I_{\ell m} \Gamma^I_{\ell m}(\xi_{ab}, f) + V(f) \sum_{\ell m} c^V_{\ell m} \Gamma^V_{\ell m}(\xi_{ab}, f) \right]$$

$$\Gamma^I_{\ell m}(\xi_{ab}, \cancel{f}) \equiv \frac{3}{4\sqrt{\pi}} \int_{S^2} \mathrm{d}^2\hat{\mathbf{n}}\, \cancel{\kappa_{ab}(f,\hat{\mathbf{n}})} Y_{\ell m}(\hat{\mathbf{n}}) \left\{ F_a^+(\hat{\mathbf{n}}) F_b^+(\hat{\mathbf{n}}) + F_a^\times(\hat{\mathbf{n}}) F_b^\times(\hat{\mathbf{n}}) \right\}$$

$$\Gamma^V_{\ell m}(\xi_{ab}, \cancel{f}) \equiv \frac{3i}{4\sqrt{\pi}} \int_{S^2} \mathrm{d}^2\hat{\mathbf{n}}\, \cancel{\kappa_{ab}(f,\hat{\mathbf{n}})} Y_{\ell m}(\hat{\mathbf{n}}) \left\{ F_a^+(\hat{\mathbf{n}}) F_b^\times(\hat{\mathbf{n}}) - F_a^\times(\hat{\mathbf{n}}) F_b^+(\hat{\mathbf{n}}) \right\}$$

angular correlation (overlap reduction) function

Angular correlation function

Taking the coordinate as

$$\hat{\mathbf{p}}_a = (0, 0, 1)\,,$$
$$\hat{\mathbf{p}}_b = (\sin\xi_{ab}, 0, \cos\xi_{ab})\,,$$
$$\hat{\mathbf{n}} = (\sin\theta\cos\phi, \sin\theta\sin\phi, \cos\theta)$$

angular pattern functions are

$$F_a^+(\hat{\mathbf{n}}) = \sin^2\left(\frac{\theta}{2}\right)\,,$$
$$F_a^\times(\hat{\mathbf{n}}) = 0\,,$$
$$F_b^+(\hat{\mathbf{n}}) = -\frac{1}{2}\frac{\sin^2\xi_{ab}(\sin^2\phi - \cos^2\theta\cos^2\phi) + \sin\xi_{ab}\cos\xi_{ab}\sin 2\theta\cos\phi - \cos^2\xi_{ab}\sin^2\theta}{1 + \sin\xi_{ab}\sin\theta\cos\phi + \cos\xi_{ab}\cos\theta}$$
$$F_b^\times(\hat{\mathbf{n}}) = -\frac{1}{2}\frac{\sin^2\xi_{ab}\cos\theta\sin 2\phi - \sin 2\xi_{ab}\sin\theta\sin\phi}{1 + \sin\xi_{ab}\sin\theta\cos\phi + \cos\xi_{ab}\cos\theta}\,.$$

Angular correlation function

The angular integral can be performed analytically.

For I mode, Anholm+, PRD (2009); Mingarelli+, PRD (2013)

$$\Gamma^I_{00}(\xi_{ab}) = \frac{1}{2} + \frac{3}{2} x_{ab} \left(\log x_{ab} - \frac{1}{6} \right) , \qquad x_{ab} \equiv \sin^2 \left(\frac{\xi_{ab}}{2} \right)$$

$$\Gamma^I_{10}(\xi_{ab}) = -\frac{\sqrt{3}}{4} (1 - x_{ab}) \left\{ 1 + 6 x_{ab} \left(1 + \frac{\log x_{ab}}{1 - x_{ab}} \right) \right\} ,$$

$$\Gamma^I_{1,-1}(\xi_{ab}) = -\Gamma^I_{11}(\xi_{ab}) = -\frac{1}{4} \sqrt{\frac{3 x_{ab}(1 - x_{ab})}{2}} \left\{ 1 + 6 x_{ab} \left(1 + \frac{\log x_{ab}}{1 - x_{ab}} \right) \right\}$$

$\Gamma^I_{00}(\xi_{ab})$ is called the Hellings-Downs curve.

For V mode, Kato & Soda, PRD (2016)

$$\Gamma^V_{10}(\xi_{ab}) = 0 ,$$

$$\Gamma^V_{1,-1}(\xi_{ab}) = \Gamma^V_{11}(\xi_{ab}) = \sqrt{\frac{3 x_{ab}(1 - x_{ab})}{2}} \left\{ 1 + \frac{3 x_{ab}}{2(1 - x_{ab})} \log x_{ab} \right\}$$

Angular correlation function

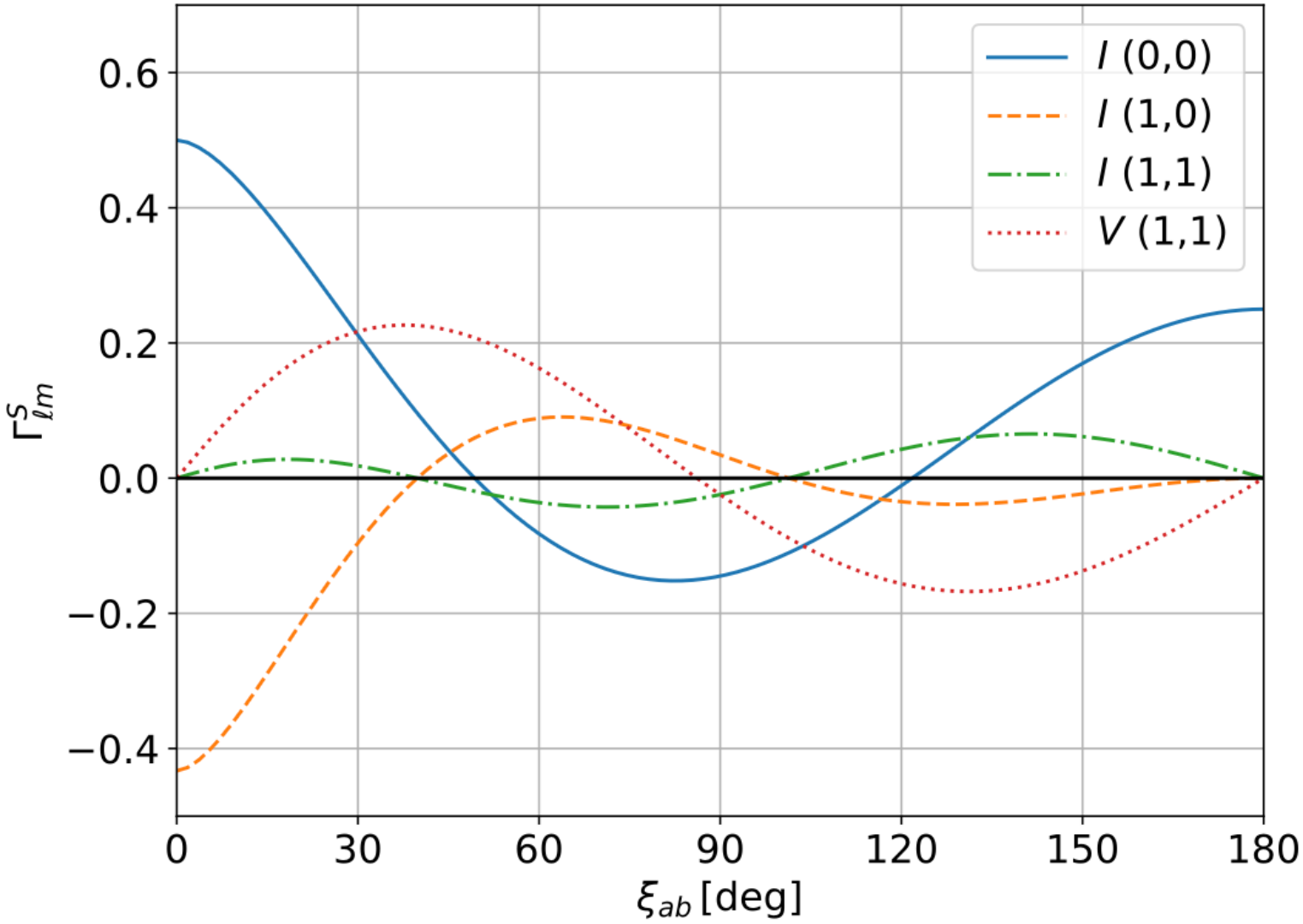

3. GW search

Correlation of time residuals

What we actually measure is not frequency changes but time residuals.

$$
\begin{aligned}
r_a(t,\hat{\mathbf{n}}) &\equiv \int_0^t z_a(t',\hat{\mathbf{n}})\mathrm{d}t' \\
&= \frac{\hat{p}_a^i \hat{p}_a^j}{2(1+\hat{\mathbf{n}}\cdot\hat{\mathbf{p}}_a)} \int_{-\infty}^{\infty} \mathrm{d}f \, \frac{1-e^{-2\pi i f t}}{2\pi i f} \tilde{h}_{ij}(f) \left\{ 1 - e^{2\pi i f \tau_a (1+\hat{\mathbf{n}}\cdot\hat{\mathbf{p}}_a)} \right\} \\
&= \int_{-\infty}^{\infty} \mathrm{d}f \, \frac{1-e^{-2\pi i f t}}{2\pi i f} \tilde{z}_a(f,\hat{\mathbf{n}}) \ .
\end{aligned}
$$

$$
\begin{aligned}
R_{ab}(t) &\equiv \langle r_a(t) r_b(t) \rangle \\
&= \frac{1}{3\sqrt{\pi}} \int_{-\infty}^{\infty} \mathrm{d}f \, \frac{1-\cos(2\pi f t)}{(2\pi f)^2} \left[I(f) \sum_{\ell m} c_{\ell m}^I \Gamma_{\ell m}^I(\xi_{ab},f) + V(f) \sum_{\ell m} c_{\ell m}^V \Gamma_{\ell m}^V(\xi_{ab},f) \right]
\end{aligned}
$$

Correlation of time residuals

For unpolarized and isotropic GWB,

$$R_{ab}(t) = \frac{2}{3}\Gamma^{I}_{00}(\xi_{ab}) \int_0^\infty \mathrm{d}f \, \frac{I(f)}{(2\pi f)^2} 2\left\{1 - \cos(2\pi f t)\right\}$$

We set $2\left\{1 - \cos(2\pi f t)\right\} \to 1$.

In practice, the frequency range of the integral is $f = [T^{-1}, \tau_{\mathrm{cad}}^{-1}]$.

T : observation time,

τ_{cad} : the cadence of observation

The frequency integral is dominated around $f = T^{-1}$.
At the frequency,

$$t : 0 \to 10\,\mathrm{yr}\,, \qquad 2\left\{1 - \cos(2\pi f t)\right\} : \; 0 \to \approx 2$$

Correlation of time residuals

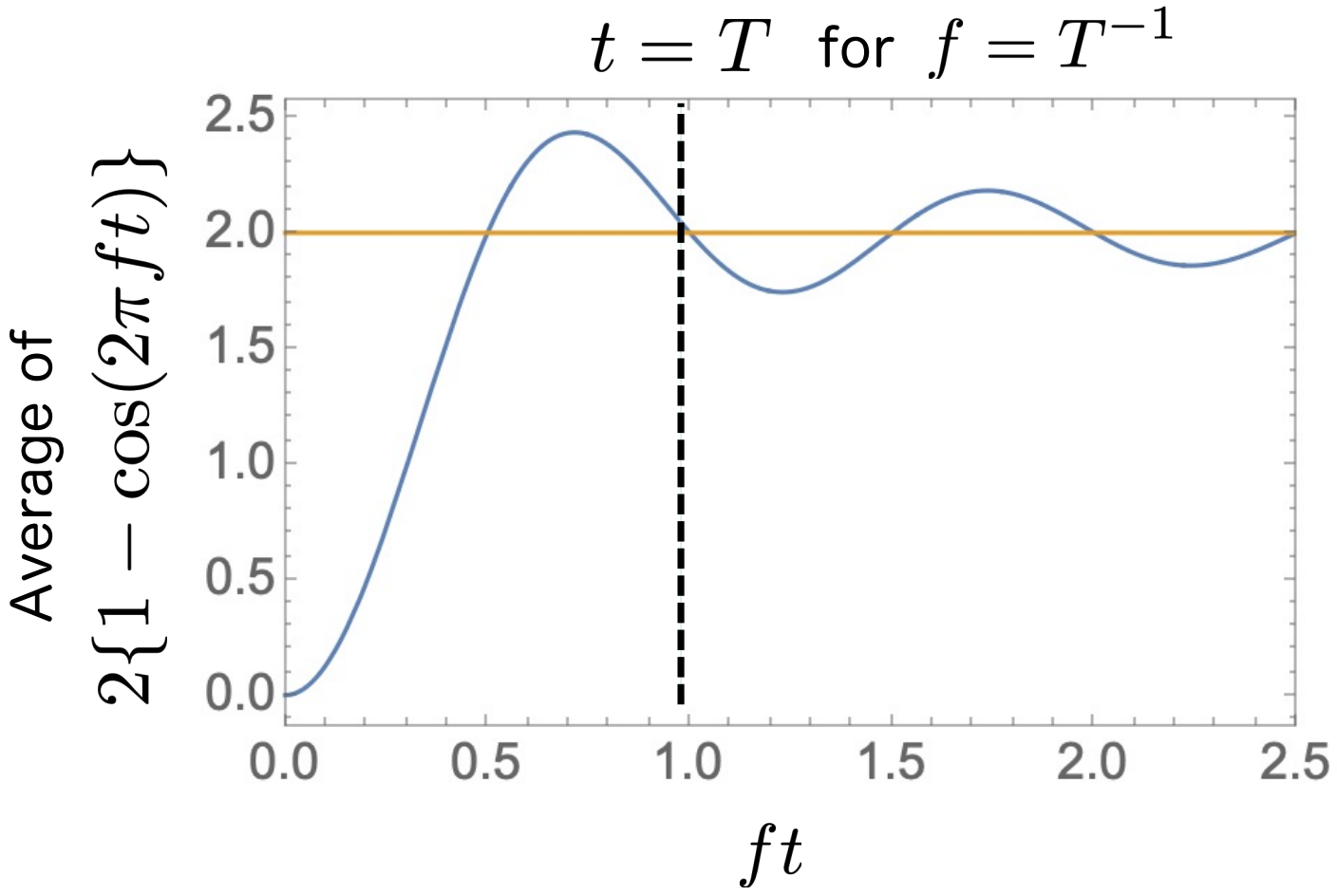

Correlation of time residuals

$$R_{ab}(t) = \frac{2}{3}\Gamma^I_{00}(\xi_{ab}) \int_0^\infty \mathrm{d}f \, \frac{I(f)}{(2\pi f)^2}$$

$$\bar{R}_{ab}(f) = \frac{2}{3}\Gamma^I_{00}(\xi_{ab}) \frac{I(f)}{(2\pi f)^2} = \Gamma^I_{00}(\xi_{ab})\Phi(f)$$

$$\Phi(f) \equiv \frac{2}{3}\frac{I(f)}{(2\pi f)^2}$$

(one-sided) power spectral density of the time residual correlation

GW power spectral density

Wiener-Khintchine's theorem

$$C(\tau) = \int_{-\infty}^{\infty} P(\omega) e^{-i\omega\tau} \mathrm{d}\omega = \int_0^\infty S(\omega) e^{-i\omega\tau} \mathrm{d}\omega$$

The Fourier transform of a correlation function is a power spectral density.

GW power spectral density

From $I(f) = S_h^{++}(f) = S_h^{\times\times}(f)$ and $h_{\rm c}^2 = 2fS_h(f)$, $\Phi(f) \equiv \frac{2}{3}\frac{I(f)}{(2\pi f)^2}$

$$\Phi(f) = \frac{h_{\rm c}^2(f)}{12\pi^2|f|^3} \longrightarrow \Phi(f) = \frac{A^2}{12\pi^2 f_{\rm ref}^{2\alpha}} f^{-\gamma} , \qquad \gamma = 3 - 2\alpha$$

$$h_{\rm c}(f) = A\left(\frac{f}{f_{\rm ref}}\right)^{\alpha}$$

GW energy density $\Omega_{\rm GW}(f) \equiv \frac{1}{\rho_{\rm c}}\frac{{\rm d}\rho_{\rm GW}(f)}{{\rm d}\log f}$ is often used.

$$\rho_{\rm GW} = \frac{1}{32\pi G} < \dot{h}_{ab}\dot{h}^{ab} >$$

$$= \frac{4}{32\pi G}\int_{f=0}^{f=\infty} {\rm d}(\log f) f (2\pi f)^2 S_h(f)$$

$$\langle \tilde{h}_A^*(f,\hat{\mathbf{n}})\tilde{h}_{A'}(f',\hat{\mathbf{n}}')\rangle \equiv \delta(f-f')\frac{1}{4\pi}\delta^2(\hat{\mathbf{n}},\hat{\mathbf{n}}')\frac{1}{2}S_h^{AA'}(f,\hat{\mathbf{n}})$$

GW power spectral density

$$\frac{\mathrm{d}\rho_{\mathrm{GW}}(f)}{\mathrm{d}\log f} = \frac{\pi}{2G} f^3 S_h(f)$$

From $\Omega_{\mathrm{GW}}(f) \equiv \frac{1}{\rho_{\mathrm{c}}} \frac{\mathrm{d}\rho_{\mathrm{GW}}(f)}{\mathrm{d}\log f}$ and $h_{\mathrm{c}}^2 = 2 f S_h(f)$,

$$\Omega_{\mathrm{GW}}(f) = \left(\frac{2\pi^2}{3H_0^2}\right) f^2 h_{\mathrm{c}}^2(f) = \left(\frac{2\pi^2}{3H_0^2}\right) A^2 f_{\mathrm{ref}}^2 \left(\frac{f}{f_{\mathrm{ref}}}\right)^{2\alpha+2}$$

For the inspiral phase driven by GW emission,

$$\alpha = -2/3, \quad \gamma = 13/3, \quad 2\alpha + 2 = 2/3$$

(This will be derived later in Part 2 of the lecture.)

Signal-to-noise ratio (SNR)

time residual signal $\zeta_a(t) = r_a(t) + \eta_a(t)$

correlation signal $Y \equiv \int_{-T/2}^{T/2} \mathrm{d}t \int_{-T/2}^{T/2} \mathrm{d}t'\, \zeta_a(t)\zeta_b(t')K_{ab}(t-t')$

optimal filter

$$\langle Y_{ab}\rangle = \int_{-\infty}^{\infty}\mathrm{d}f \int_{-\infty}^{\infty}\mathrm{d}f' \int_{-\infty}^{\infty}\mathrm{d}f'' \int_{-T/2}^{T/2}\mathrm{d}t \int_{-T/2}^{T/2}\mathrm{d}t'\, e^{-2\pi i f''(t-t')}e^{2\pi i f t}e^{-2\pi i f' t'}$$
$$\times\langle \tilde{r}_a^*(f)\tilde{r}_b(f')\rangle \tilde{K}_{ab}(f'')$$
$$= \frac{T}{2}\Gamma_{00}^I(\xi_{ab})\int_{-\infty}^{\infty}\mathrm{d}f\,\Phi(f)\tilde{K}_{ab}(f)$$

$$\langle Y_{ab}^2\rangle = \frac{T}{4}\int_{-\infty}^{\infty}\mathrm{d}f\,\{\Phi(f)+2P_{\eta,a}(f)\}\{\Phi(f)+2P_{\eta,b}(f)\}|\tilde{K}_{ab}(f)|^2$$

$$\mathrm{SNR} \equiv \frac{\langle Y_{ab}\rangle}{\sqrt{\mathrm{Var}[Y_{ab}]\rangle}} \qquad \langle \tilde{\eta}_a^*(f)\tilde{\eta}_a(f')\rangle = \delta(f-f')P_{\eta,a}(f)$$

Signal-to-noise ratio (SNR)

Defining the inner product,

$$(A,B)_{ab} \equiv \int_{-\infty}^{\infty} df\, A^*(f) B(f) \left\{\Phi(f) + P_{\eta,a}(f)\right\} \left\{\Phi(f) + P_{\eta,b}(f)\right\}$$

the expectation value and variance of the signal are written as

$$\langle Y_{ab} \rangle = \frac{T}{2} \Gamma^I_{00}(\xi_{ab}) \left(\tilde{K}_{ab}(f), \frac{\Phi(f)}{\left\{\Phi(f) + 2P_{\eta,a}(f)\right\} \left\{\Phi(f) + 2P_{\eta,b}(f)\right\}} \right)_{ab}$$

$$\langle Y^2_{ab} \rangle = \frac{T}{4} \left(\tilde{K}_{ab}(f), \tilde{K}_{ab}(f) \right)_{ab} ,$$

$$\tilde{K}_{ab}(f) = K_0 \frac{\Phi(f)}{\left\{\Phi(f) + 2P_{\eta,a}(f)\right\} \left\{\Phi(f) + 2P_{\eta,b}(f)\right\}}$$

$$\mathrm{SNR}_{ab} = \Gamma^I_{00}(\xi_{ab}) \left[2T \int_0^{\infty} df \frac{\Phi^2(f)}{\left\{\Phi(f) + 2P_{\eta,a}(f)\right\} \left\{\Phi(f) + 2P_{\eta,b}(f)\right\}} \right]^{1/2}$$

Parameter inference

likelihood function

Lentati, Alexander, Hobson, PRD (2013)
van Haasteren & Vallisneri, PRD (2014)

$$p(\boldsymbol{\delta t}|\boldsymbol{c},\boldsymbol{\epsilon}) = \frac{1}{\sqrt{\det(2\pi \boldsymbol{C})}} \exp\left[-\frac{1}{2}\boldsymbol{r}^T \boldsymbol{C}^{-1}\boldsymbol{r}\right]$$

$$\boldsymbol{r} = \boldsymbol{\delta t} - \underline{\boldsymbol{F c}} - \underline{\boldsymbol{M \epsilon}}$$

theoretical model timing model uncertainties

$\boldsymbol{\delta t}$: time residual data

$\boldsymbol{F}$: Fourier basis (cosines & sines at $f_i = i/T$)

$\boldsymbol{c}$: Fourier amplitude

$$\langle c_{ai} c_{bj} \rangle = \delta_{ij} \left\{ \delta_{ab} \varphi_{ai} + \delta_{ab} \Phi_i^{\mathrm{CURN}} + \Gamma(\xi_{ab}) \Phi_i^{\mathrm{HD}} \right\}$$

a, b : pulsars, i, j : Fourier components

$\boldsymbol{M}$: design matrix basis, $\boldsymbol{\epsilon}$: coefficients

Summary of Part 1

- The period of millisecond pulsars is very stable and can be used for GW detection.
- Time residuals of pulses are modeled by GW signal + timing model + noise model.
- GW signals shows a characteristic correlation between pulsars, namely, the Hellings-Downs curve.
- A GW spectrum from massive BHs is parameterized by

$$\Phi(f) = \frac{h_{\rm c}^2(f)}{12\pi^2|f|^3} \longrightarrow \Phi(f) = \frac{A^2}{12\pi^2 f_{\rm ref}^{2\alpha}} f^{-\gamma}\,, \qquad \gamma = 3 - 2\alpha$$

$$h_{\rm c}(f) = A\left(\frac{f}{f_{\rm ref}}\right)^{\alpha}$$

$$\Omega_{\rm GW}(f) = \left(\frac{2\pi^2}{3H_0^2}\right) f^2 h_{\rm c}^2(f) = \left(\frac{2\pi^2}{3H_0^2}\right) A^2 f_{\rm ref}^2 \left(\frac{f}{f_{\rm ref}}\right)^{2\alpha+2}$$

Part 2:
GW detection and GWB from supermassive black-hole binaries

4. Observational results

GWB evidence

- On June 29, 2023, four PTA groups (EPTA+InPTA, NANOGrav, PPTA, CPTA) announced that the "evidence" of a GWB was detected.
- The Hellings-Downs correlation has been detected with 2-4σ significance.
- The signal is consistent with a GWB from SMBH binaries, but the origin is not identified yet.

Data set

Agazie+ (IPTA), ApJ (2024)

EPTA: 10.3 yr data for 25 pulsars

InPTA: 3.5 yr data for 10 overlapping pulsars

NANOGrav: 15 yr data for 68 pulsars

PPTA: 18 yr data for 32 pulsars

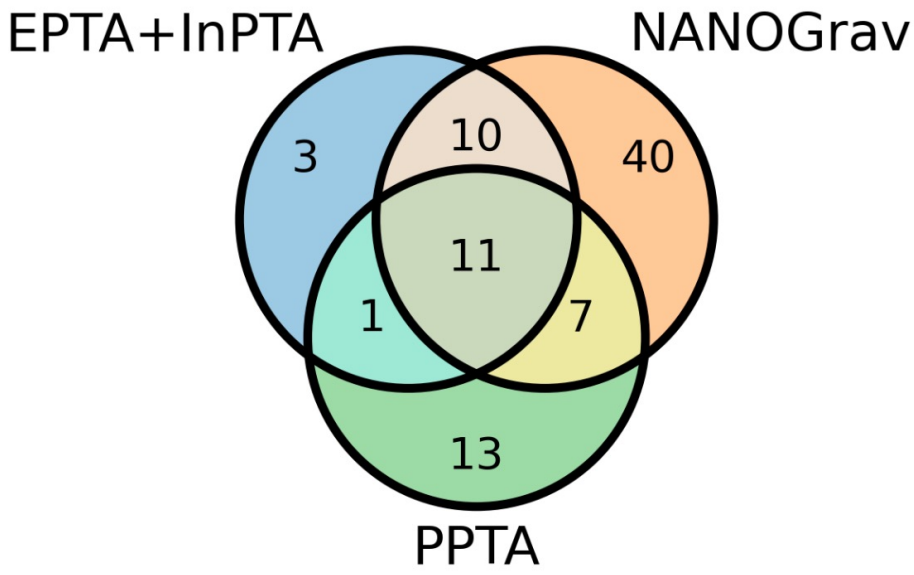

GW amplitude spectrum

$$\mathrm{RMS}_i \equiv \left[\int_{\Delta f_i} \Phi(f)\mathrm{d}f\right]^{1/2}$$

Assuming the Hellings-Downs curve (response).

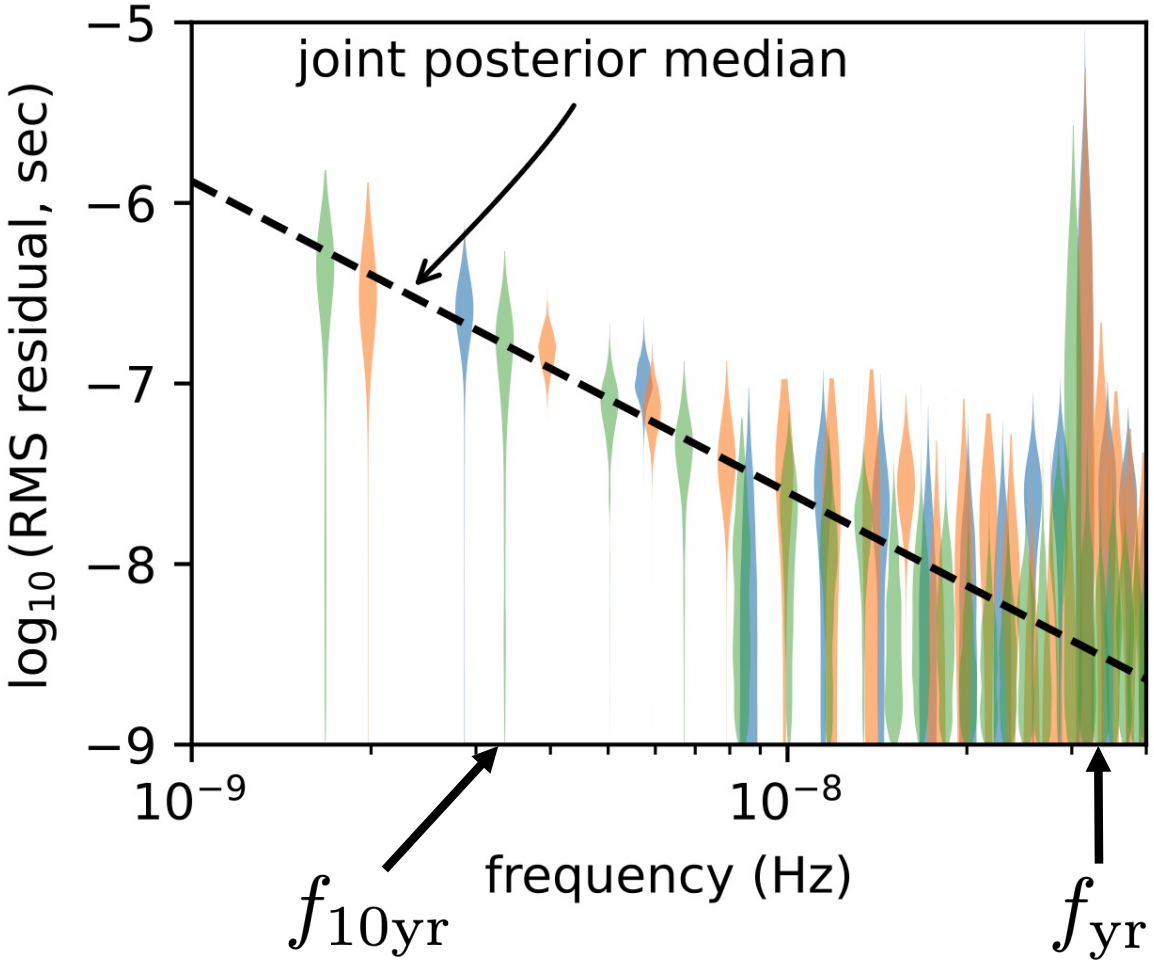

EPTA+InPTA
NANOGrav
PPTA

Noise model:

1. intrinsic red noise
2. interstellar DM variation
3. deterministic solar wind
4. common uncorrelated red noise (CURN) with $\gamma_{\mathrm{CURN}} = 13/3$

Model parameters

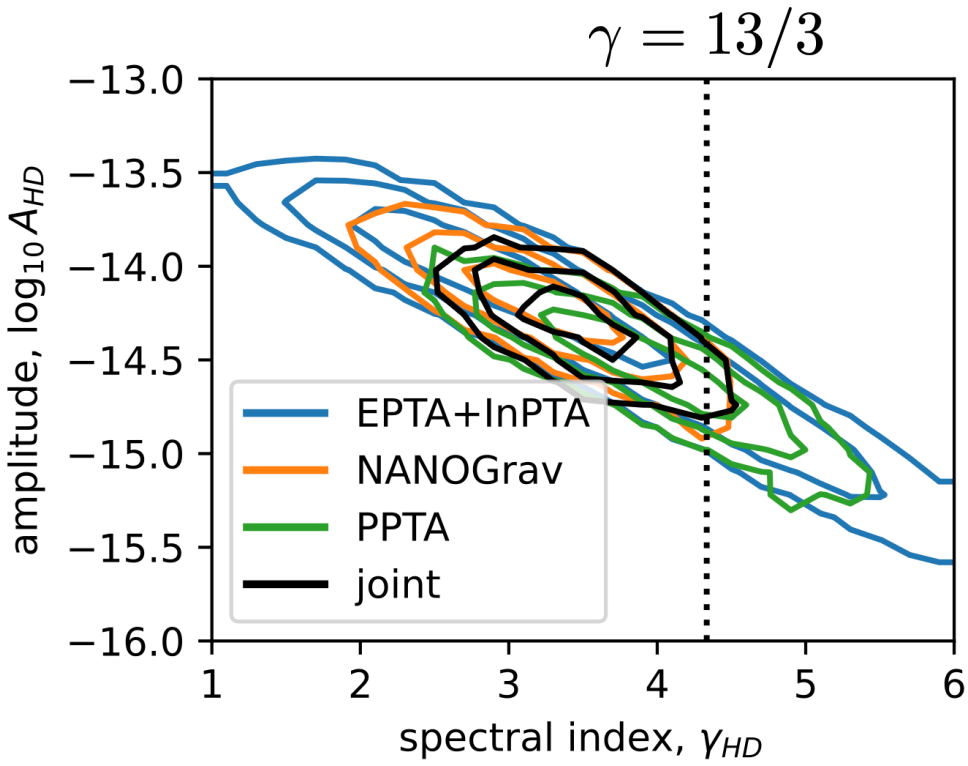

$$\Phi(f) = \frac{A^2}{12\pi^2 f_{\rm ref}^{2\alpha}} f^{-\gamma}$$

What is plotted in the previous slide.

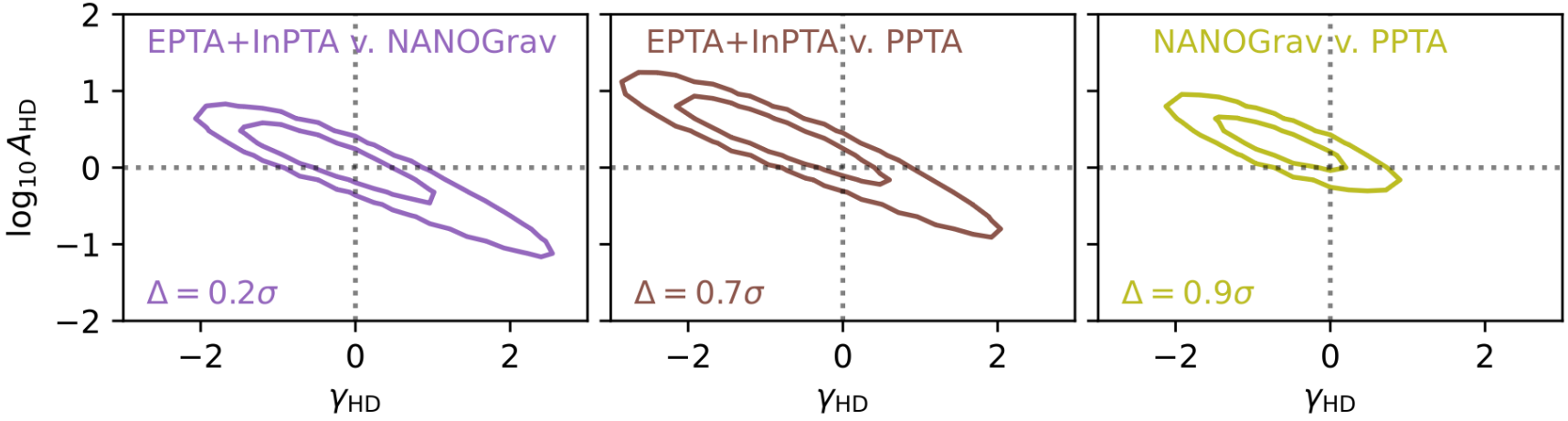

Hellings-Downs curve

Taylor, arXiv:2511.08966

Agazie *et al* 2023 *ApJL* 951 L8

3σ-4σ

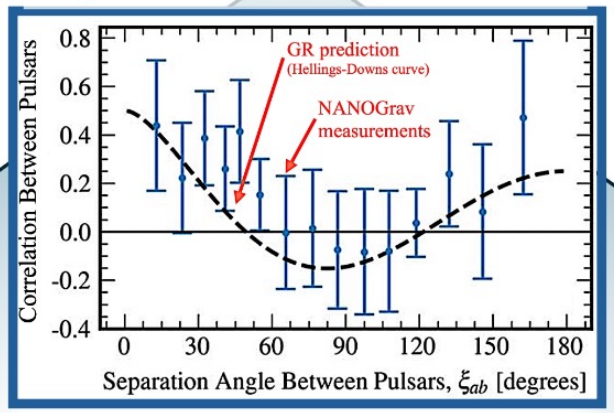

~3σ

Antoniadis et al 2023 A&A 678, A50

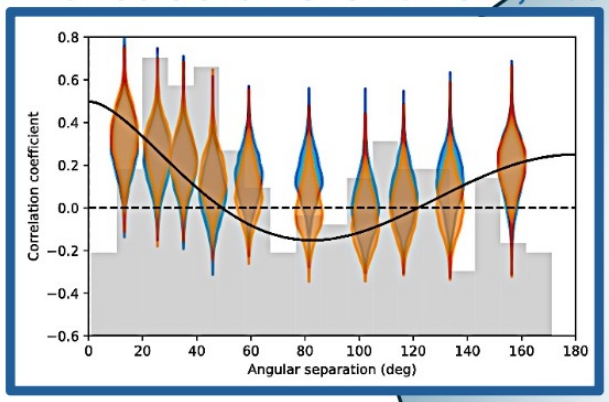

~2σ

Reardon *et al* 2023 *ApJL* 951 L6

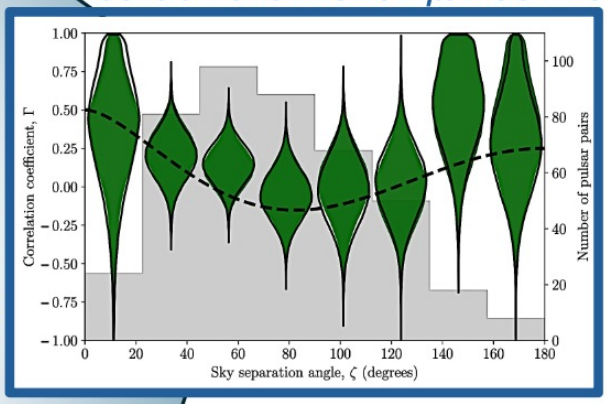

NANOGrav

EPTA

InPTA

Indian Pulsar Timing Array

PPTA

MPTA

CPTA

~3σ

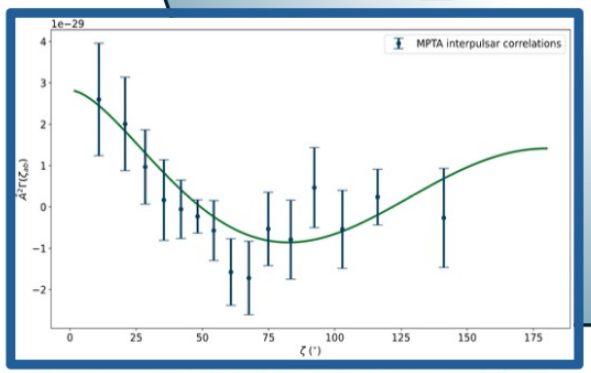

Miles et al 2025 MNRAS 536 2

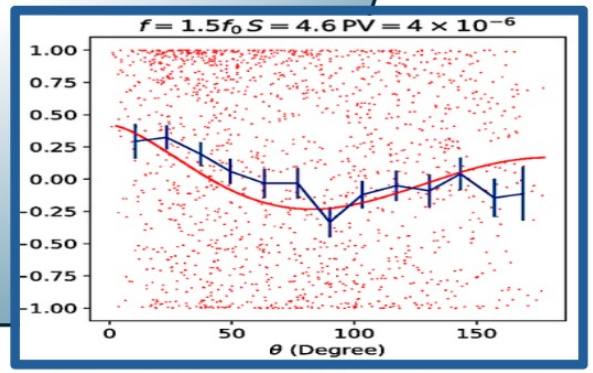

Xu et al 2023 RAA 23 075024

~4.6σ

Sensitivity

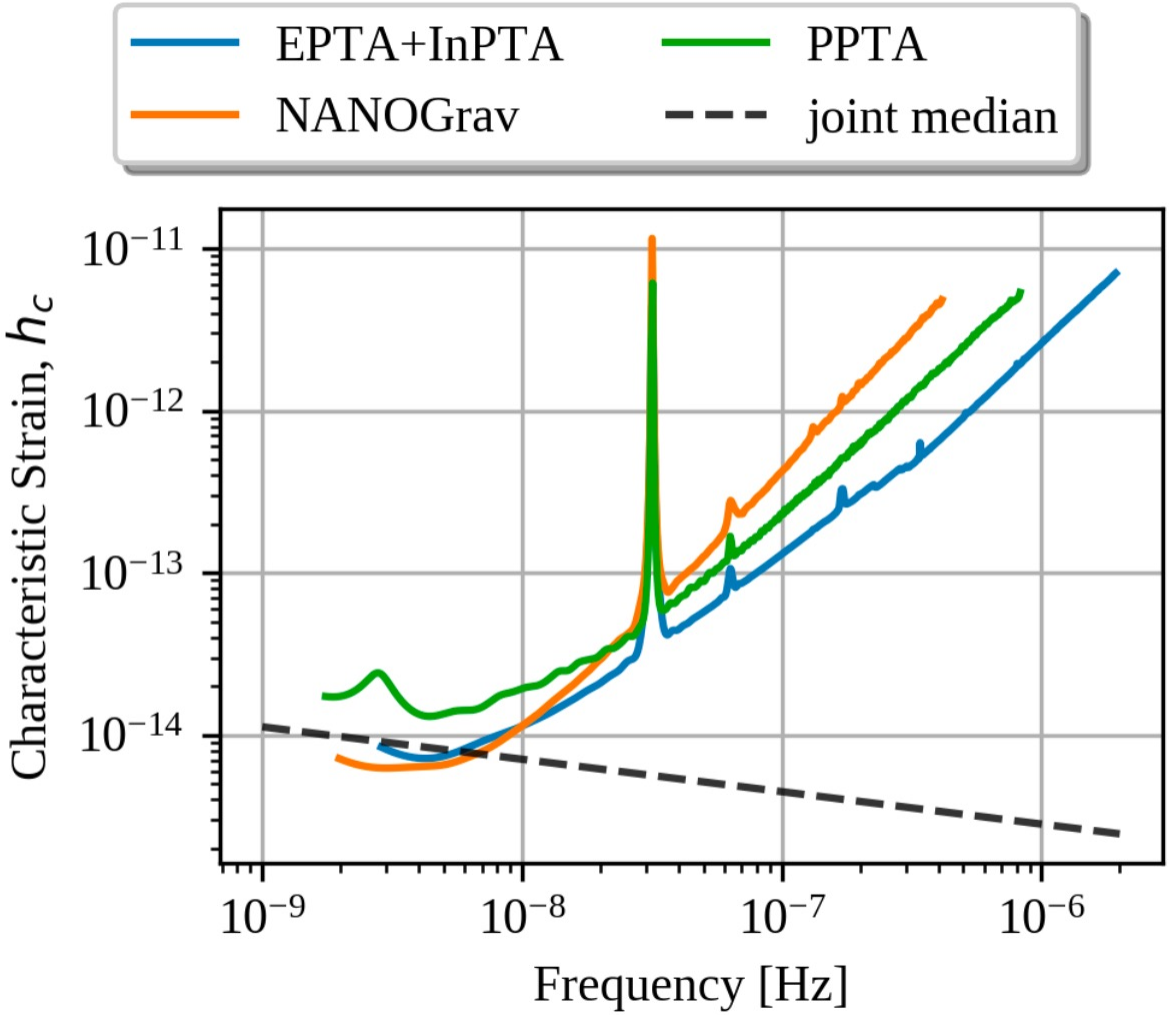

$$\Phi(f) = \frac{h_c^2(f)}{12\pi^2|f|^3}$$

- NANOGrav is the best at low freq. due to the longer data set and less noise.
- EPTA+InPTA is the best at high freq. due to high obs cadence (~3 days).
- PPTA's cadence is ~7 days. NANOGrav's cadence is 30 or 14 days.

SNR

$$\mathrm{SNR}_{ab} = \Gamma^{I}_{00}(\xi_{ab}) \left[2T \int_0^\infty df \frac{\Phi^2(f)}{\{\Phi(f) + 2P_{\eta,a}(f)\}\{\Phi(f) + 2P_{\eta,b}(f)\}} \right]^{1/2}$$

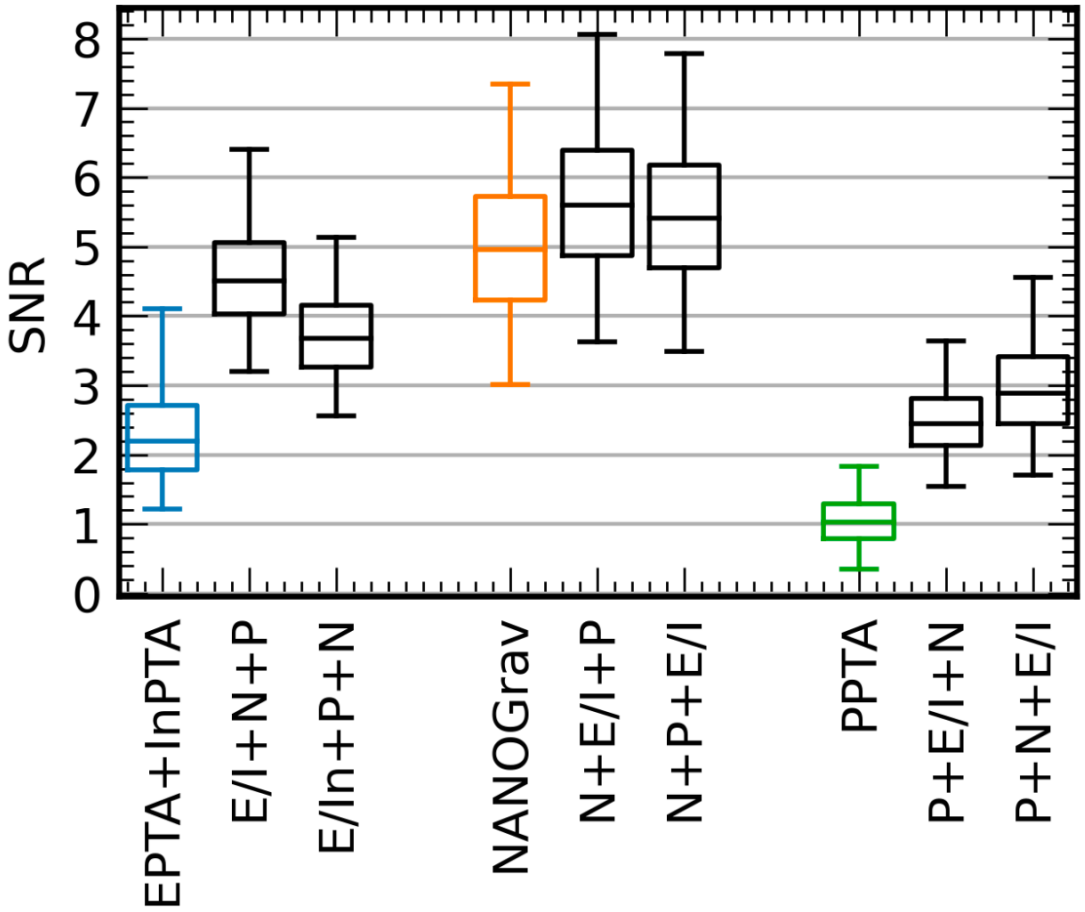

Box: 25 – 75 %
Bar: 2.5 - 97.5 %

Note that the SNRs are different from those from individual searches, because of the noise models used.

Upper limit on GWBs

ϵ : error of time residuals, T : observation time

$$h_{\rm c}(f_*) \sim \frac{\epsilon}{T}, \qquad f_* \equiv \frac{1}{T}$$

Typically, $\epsilon \sim 100\,\mathrm{nsec}$, $T \sim 10\,\mathrm{yr}$

ideally sensitive down to $h_{\rm c} \sim 10^{-16}$ at $f \sim 3 \times 10^{-9}\,\mathrm{Hz}$

For $f > f_*$, $h_{\rm c}(f) \sim \frac{\epsilon}{P}\sqrt{\frac{P}{T}}$ P : GW period

From $h_0^2 \Omega_{\rm GW} \propto f^2 h_c^2$, $\Omega_{\rm GW}(f) < \Omega_{\rm GW}(f_*) \left(\frac{f}{f_*}\right)^3$

Demorest+ (NANOGrav), ApJ (2013)

for $\gamma = 13/3$ (95% CL)

$$h_0^2 \Omega_{\rm GW}(f_{\rm yr}) < 3.1 \times 10^{-8} \qquad \text{at} \quad f_{\rm yr} = 3.2 \times 10^{-8}\,\mathrm{Hz}$$

Upper limit on GWBs

Liu & Chen, arXiv:2602.14014 (2026)

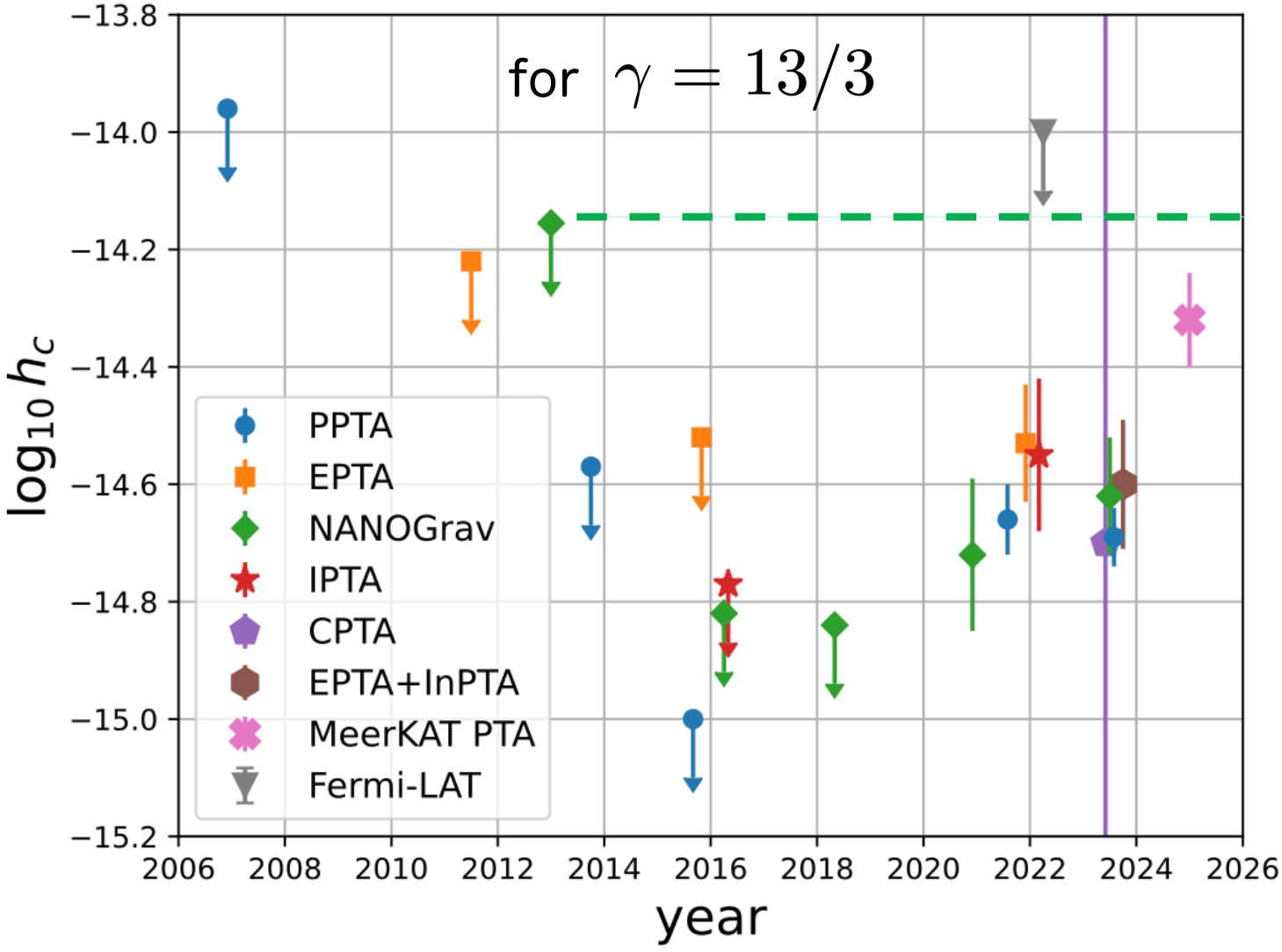

5. GW emission from a BH binary

GW-driven binary inspirals

For a circular binary, $\omega_{\rm GW} = 2\,\omega_{\rm s}$

GW orbital energy $$E_{\rm orbit} = -\frac{G m_1 m_2}{2\bar{R}} = -\left(\frac{G^2 \mathcal{M}_{\rm c}^5 \omega_{\rm GW}^2}{32}\right)^{1/3}$$

chirp mass $\mathcal{M}_{\rm c} \equiv \dfrac{(m_1 m_2)^{3/5}}{(m_1+m_2)^{1/5}}$ Kepler's law $\omega_{\rm s}^2 = GM/\bar{R}^3$

GW luminosity $$L_{\rm GW} = \frac{32}{5}\frac{G\mu^2 \bar{R}^4 \omega_{\rm s}^6}{c^5} = \frac{2^{5/3}}{5}\frac{G^{7/3}\mu^2 M^{4/3}\omega_{\rm GW}^{10/3}}{c^5}$$

From $\dot{E}_{\rm orbit} = -L_{\rm GW}$, $$\dot{f}_{\rm GW} = \frac{96}{5}\pi^{8/3}\left(\frac{G\mathcal{M}_{\rm c}}{c^3}\right)^{5/3} f_{\rm GW}^{11/3}$$

integrating

τ : time to merger $$f_{\rm GW} = \frac{1}{\pi}\left(\frac{5}{256}\frac{1}{\tau}\right)^{3/8}\left(\frac{G\mathcal{M}_{\rm c}}{c^3}\right)^{-5/8}$$

GW-driven binary inspiral

From the formula in the previous slide,

$$f_{\rm GW} \approx 1.74\,{\rm nHz} \left(\frac{10^7\,{\rm M}_\odot}{\mathcal{M}_{\rm c}}\right)^{5/8} \left(\frac{10^{10}\,{\rm yr}}{\tau}\right)^{3/8}$$

For a SMBH binary with $\mathcal{M}_{\rm c} \geq 10^7\,M_\odot$, the pulsar timing band is GW-driven (Binaries can merger in the cosmic time).

Using the Kepler's law $\omega_{\rm s}^2 = GM/\bar{R}^3$, $f_{\rm 15yr} = (15\,{\rm yr})^{-1} \approx 2.11\,{\rm nHz}$

$$f_{\rm GW} \approx 1.63\,{\rm nHz} \left(\frac{\rm M}{2\times 10^9\,{\rm M}_\odot}\right)^{1/2} \left(\frac{0.07\,{\rm pc}}{\bar{\rm R}}\right)^{3/2}$$

For $\bar{R} \lesssim 0.07\,{\rm pc}$, SMBH binaries are in the pulsar timing band and GW-driven.

For $\bar{R} \gtrsim 0.07\,{\rm pc}$, SMBH binaries need an efficient mechanism to push them to the pulsar timing band (subparsec problem).

Life cycle of a SMBH binary

Burke-Spolaor+, A&A Review (2019)

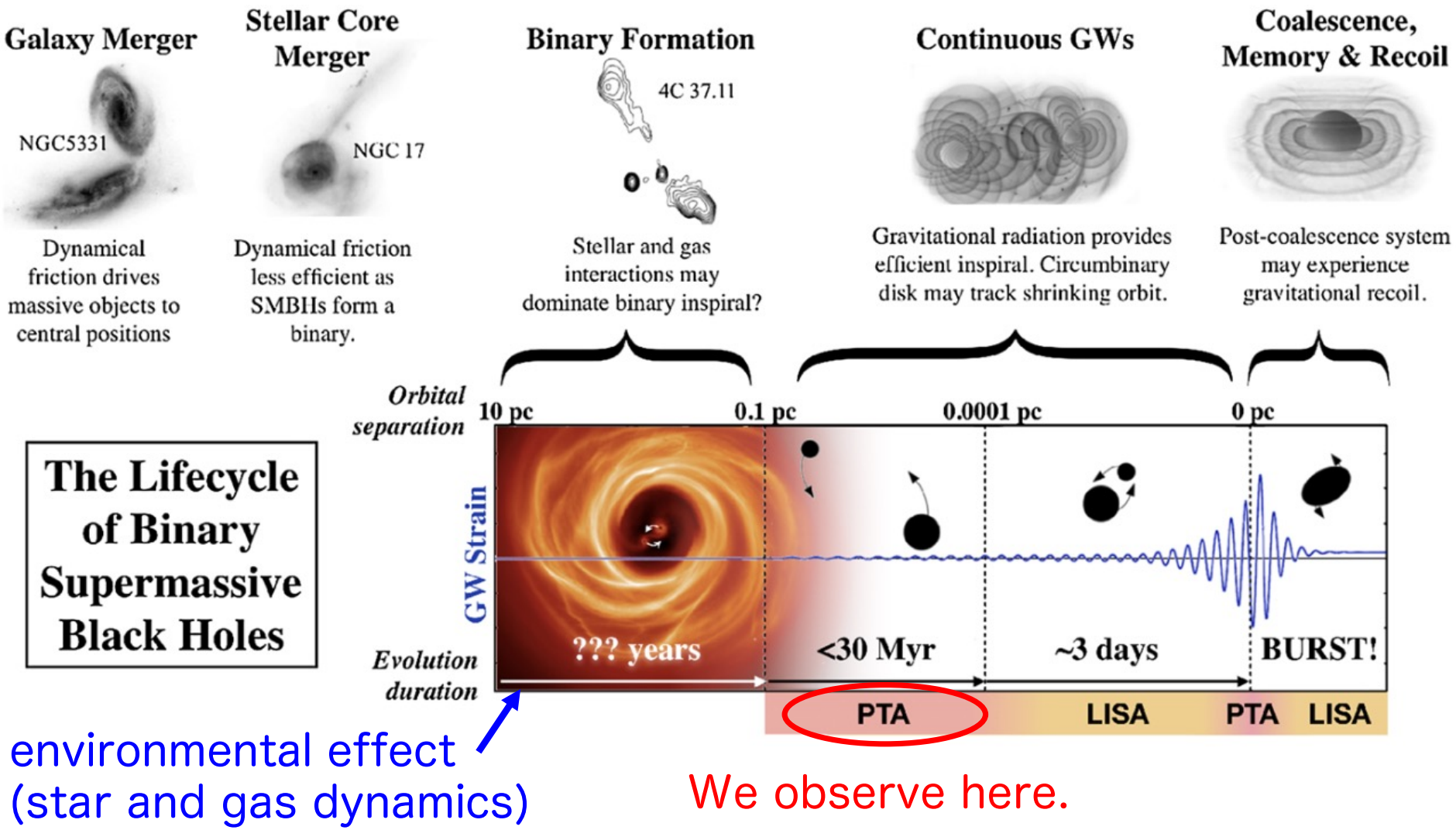

GW spectral index

For a circular binary, GW waveforms (Newtonian order) are

$$\tilde{h}_+(f) = \sqrt{\frac{5}{24\,\pi^{4/3}}}\frac{c}{r}\left(\frac{G\mathcal{M}_{\rm c}}{c^3}\right)^{5/6} f^{-7/6}\,\frac{1+\cos^2\iota}{2}\,e^{i\Psi_+}\ ,$$

$$\tilde{h}_\times(f) = \sqrt{\frac{5}{24\,\pi^{4/3}}}\frac{c}{r}\left(\frac{G\mathcal{M}_{\rm c}}{c^3}\right)^{5/6} f^{-7/6}\,\cos\iota\,e^{i\Psi_\times}\ ,$$

From $\langle \tilde{h}^*_A(f,\hat{\mathbf{n}})\tilde{h}_{A'}(f',\hat{\mathbf{n}}')\rangle \equiv \delta(f-f')\frac{1}{4\pi}\delta^2(\hat{\mathbf{n}},\hat{\mathbf{n}}')\frac{1}{2}S_h^{AA'}(f,\hat{\mathbf{n}})$

$$S_h \propto f^{-7/3} \longrightarrow h_{\rm c} \propto f^{-2/3}$$

$$h_{\rm c}^2 = 2fS_h(f)$$

$$h_{\rm c}(f) = A\left(\frac{f}{f_{\rm ref}}\right)^{\alpha}$$
$$\alpha = -2/3$$

$$\gamma = 3 - 2\alpha$$

$$\Phi(f) = \frac{A^2}{12\pi^2 f_{\rm ref}^{2\alpha}} f^{-\gamma}$$
$$\gamma = 13/3$$

Effect of eccentricity

For an eccentric orbit ($0 < e < 1$)

$$L_{\rm GW} = \frac{32}{5}\frac{G\mu^2 a^4 \omega_{\rm s0}^6}{c^5} F(e), \qquad F(e) = \frac{1}{(1-e^2)^{7/2}}\left(1 + \frac{73}{24}e^2 + \frac{37}{96}e^4\right)$$

difference from a circular case

$$\omega_{\rm s0}^2 \equiv \frac{GM}{a^3}$$

For a circular orbit ($e = 0$),

$$a = \bar{R},\ \omega_{\rm s0} = \omega_{\rm s}$$

Eccentricity increases GW luminosity and accelerate the orbital shrinkage and the frequency evolution of a binary.

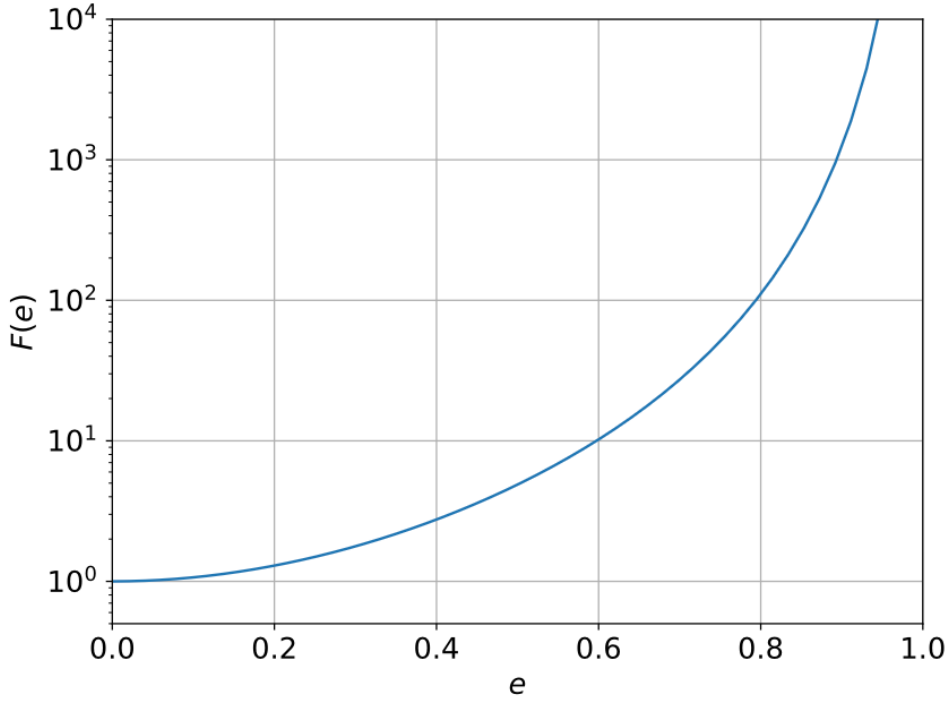

Effect of environment

Dynamics of gas and stars affect binary hardening.

However, the effect is described by dozens of free parameters, which are highly degenerated in the parameter estimation.

Phenomenological models:

- Model for the orbital separation of a binary

$$\frac{1}{a}\frac{\mathrm{d}a}{\mathrm{d}t} \propto a^{-\nu_{\mathrm{inner}}} \quad \text{for } a \ll a_{\mathrm{c}} \quad , \quad \frac{1}{a}\frac{\mathrm{d}a}{\mathrm{d}t} \propto a^{-\nu_{\mathrm{outer}}} \quad \text{for } a \gg a_{\mathrm{c}}$$

- Model for the merging timescale of a binary

$$\tau = \tau_0 \left(\frac{M}{10^{11}\, M_\odot} \right)^{\alpha_\tau} (1+z)^{\beta_\tau} q^{\gamma_\tau}$$

6. GWB from supermassive BH binaries

GWB from compact binaries

$$h_{\rm c}^2(f) = \frac{4G}{\pi c^2 f^2} \int_0^\infty {\rm d}z \int_0^\infty {\rm d}\boldsymbol{\theta} \frac{{\rm d}^2 n}{{\rm d}z\,{\rm d}\boldsymbol{\theta}} \frac{1}{1+z} \frac{{\rm d}E_{\rm GW}(f_{\rm s},\boldsymbol{\theta})}{{\rm d}\log f_{\rm s}}$$

e.g. Phinney, astro-ph/0108028 (2001)

$f_{\rm s} = (1+z)f$: GW frequency in the source frame

GW energy spectrum in the source frame

$$\frac{{\rm d}E_{\rm GW}(f_{\rm s},\boldsymbol{\theta})}{{\rm d}\log f_{\rm s}} = 4\pi r^2 \frac{\pi c^3}{2G} f_s^3 \left[h_+^2(f_{\rm s},\boldsymbol{\theta}) + h_\times^2(f_{\rm s},\boldsymbol{\theta})\right]$$

determined by GR

binary parameters $\boldsymbol{\theta} = \{\mathcal{M}_{\rm c}, q, e, \cdots\}$

comoving number density per redshift per binary parameters

$$\frac{{\rm d}^2 n}{{\rm d}z\,{\rm d}\boldsymbol{\theta}}$$

determined by astrophysical population

GWB from supermassive BHs

Ellis et al., A&A (2023)

BH merger rate

halo merger rate

$$\frac{\mathrm{d}R_{\mathrm{BH}}}{\mathrm{d}m_1\mathrm{d}m_2} = \int \mathrm{d}M_1\mathrm{d}M_2\, p_{\mathrm{merg}}(m_1,m_2)p_{\mathrm{occ}}(m_1|M_1)p_{\mathrm{occ}}(m_2|M_2)\frac{\mathrm{d}R_{\mathrm{h}}}{\mathrm{d}M_1\mathrm{d}M_2}$$

$$\approx p_{\mathrm{BH}}\frac{\mathrm{d}M_1}{\mathrm{d}m_1}\frac{\mathrm{d}M_2}{\mathrm{d}m_2}\frac{\mathrm{d}R_{\mathrm{h}}}{\mathrm{d}M_1\mathrm{d}M_2}$$

from Illustris simulation

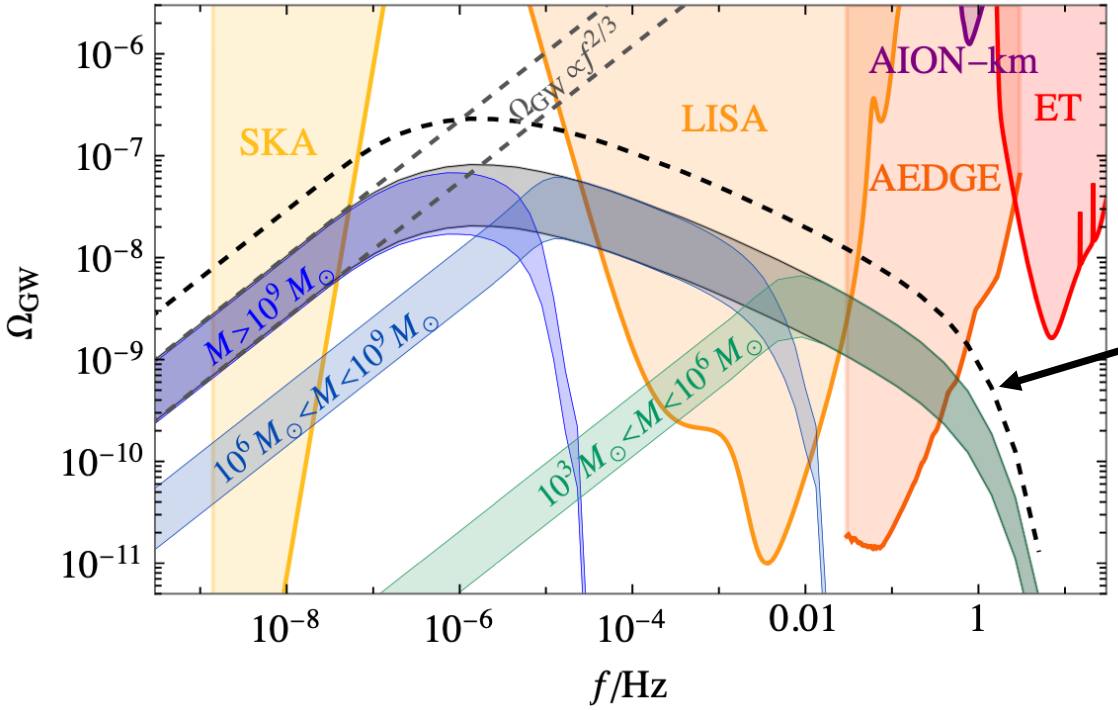

from the observation of IPTA

$$p_{\mathrm{BH}} = 0.17^{+0.18}_{-0.08}$$

$$p_{\mathrm{BH}} = 1$$

The largest contribution to the pulsar timing band comes from SMBH binaries with $M > 10^9\,M_\odot$.

Astrophysical complications

Kelley, arXiv:2505.00797 (2025)

$$\left(\frac{da}{dt}\right) = \left(\frac{da}{dt}\right)_{\rm GW} + \left(\frac{da}{dt}\right)_{\rm env}$$

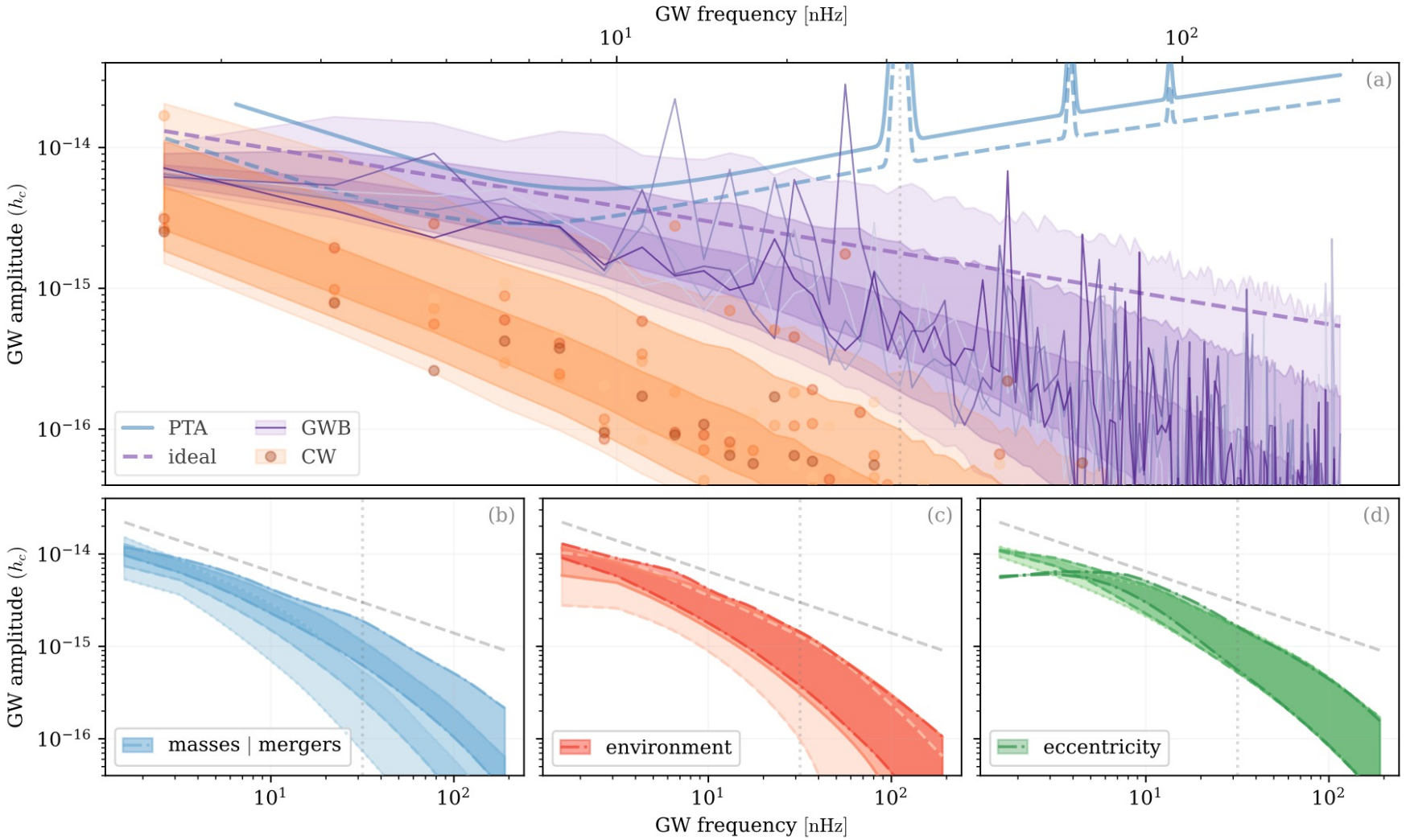

Interpretation of the observational results

Antoniadis+ (EPTA & InPTA), A&A (2024)

$$\frac{\mathrm{d}^5 n}{\mathrm{d}z\,\mathrm{d}m_1\,\mathrm{d}q\,\mathrm{d}e\,\mathrm{d}\omega_{\mathrm{s0}}}$$

- galaxy mass function
- pair fraction
- galaxy pair merger timescale
- SMBH-host galaxy relation
- SMBH accretion during merger

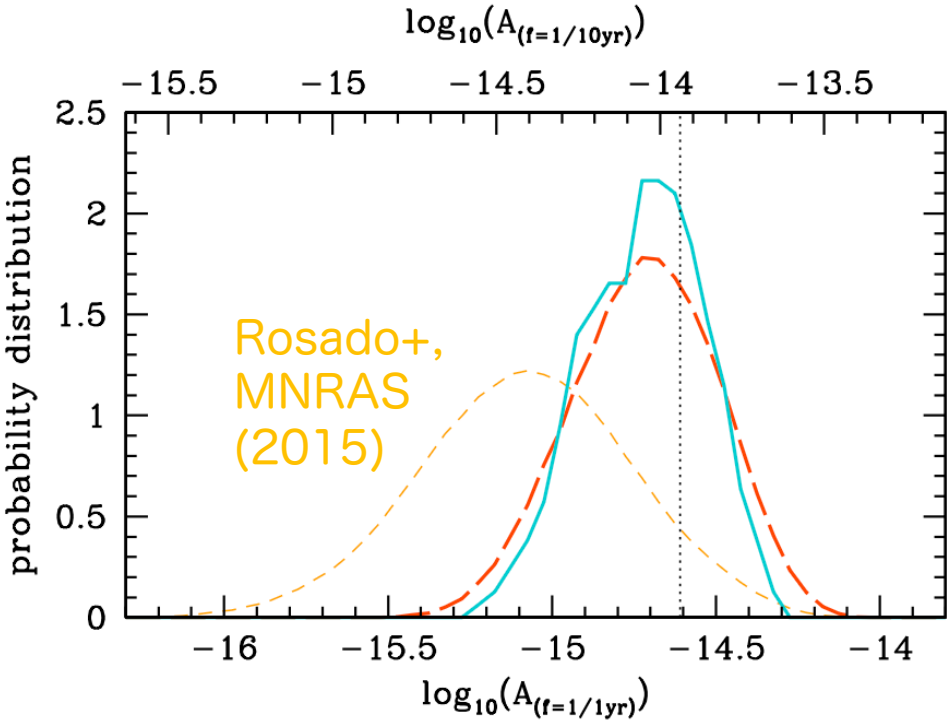

subgroup of RSG15 (108 models)

X

eccentricity (0, 0.1, ⋯, 0.9)

X

stellar density profile (0.1, 1, 10 times)

⇩

3240 models

Interpretation of the observational results

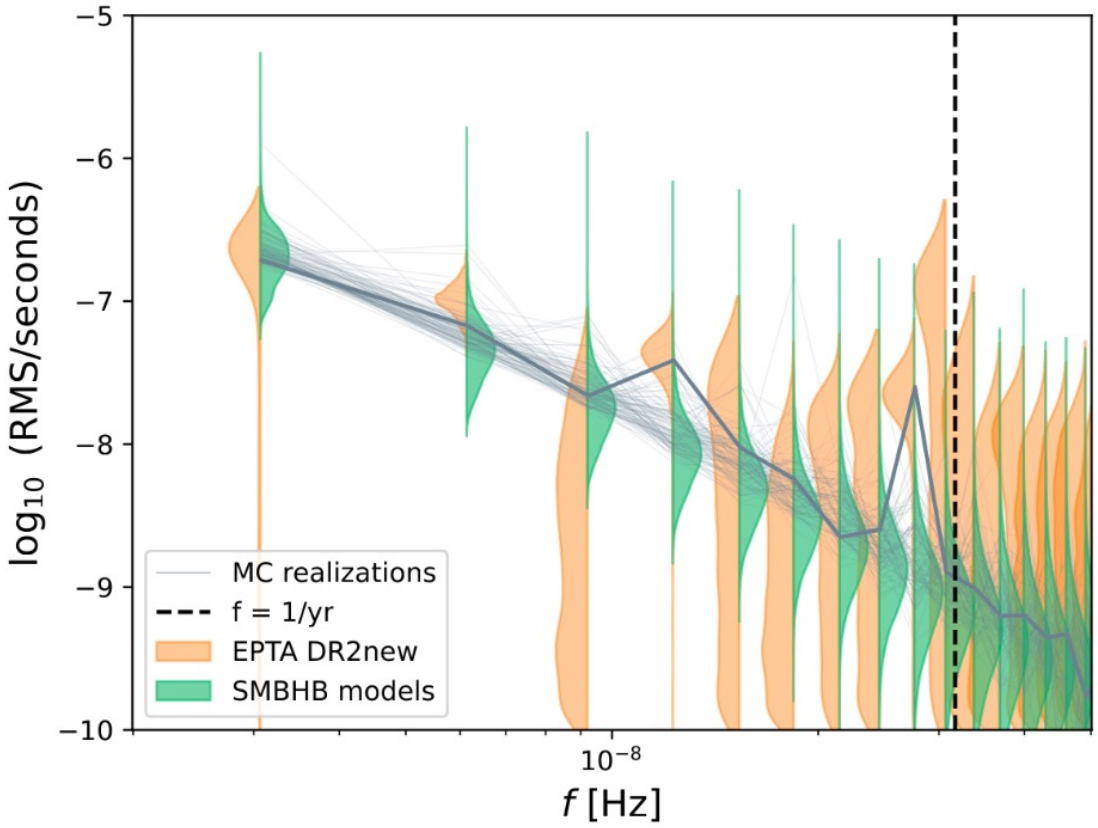

- A few low freq. bins are in good agreement with observations, at which the sensitivity of the pulsar timing is best.
- The amplitude distributions are highly non-Gaussian, because a small number of loud signals contribute.

Interpretation of the observational results

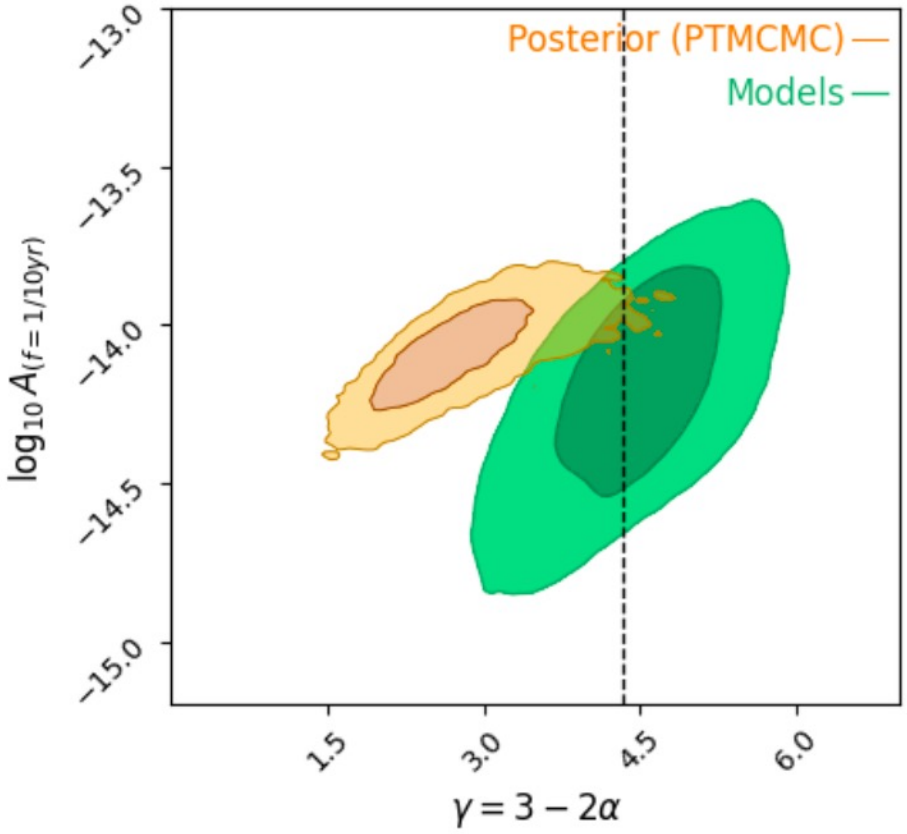

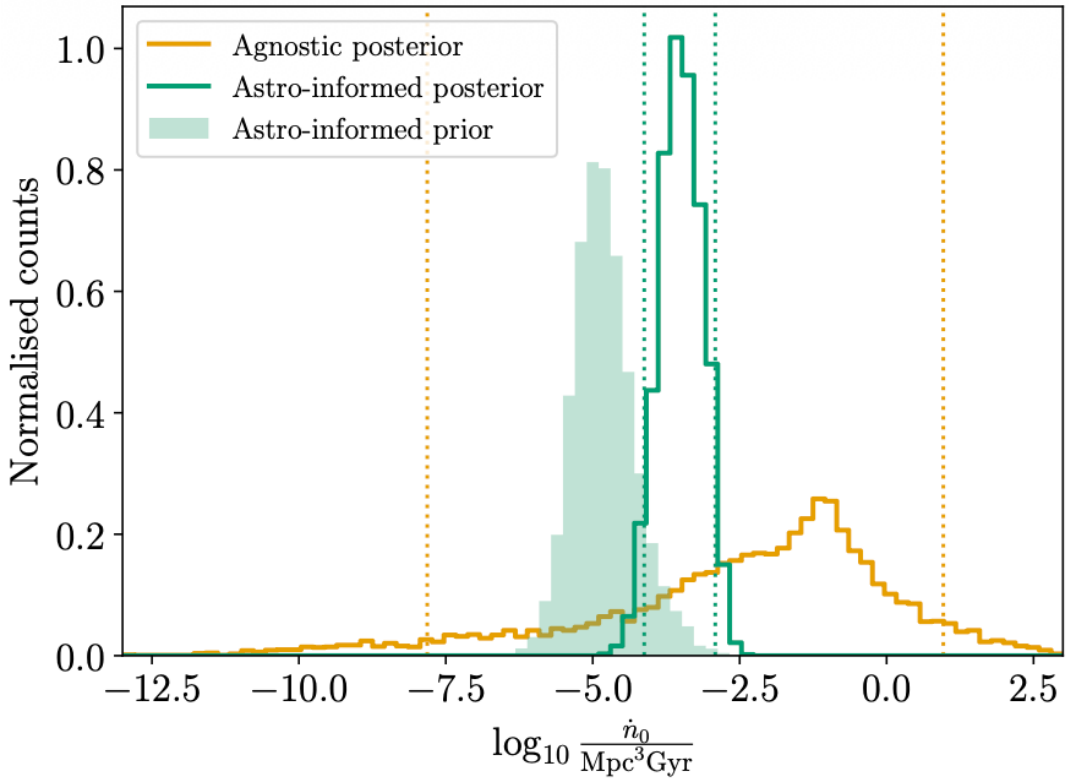

For the amplitude or the merger rate, the upper edge of the astrophysical prior is preferred.

Interpretation of the observational results

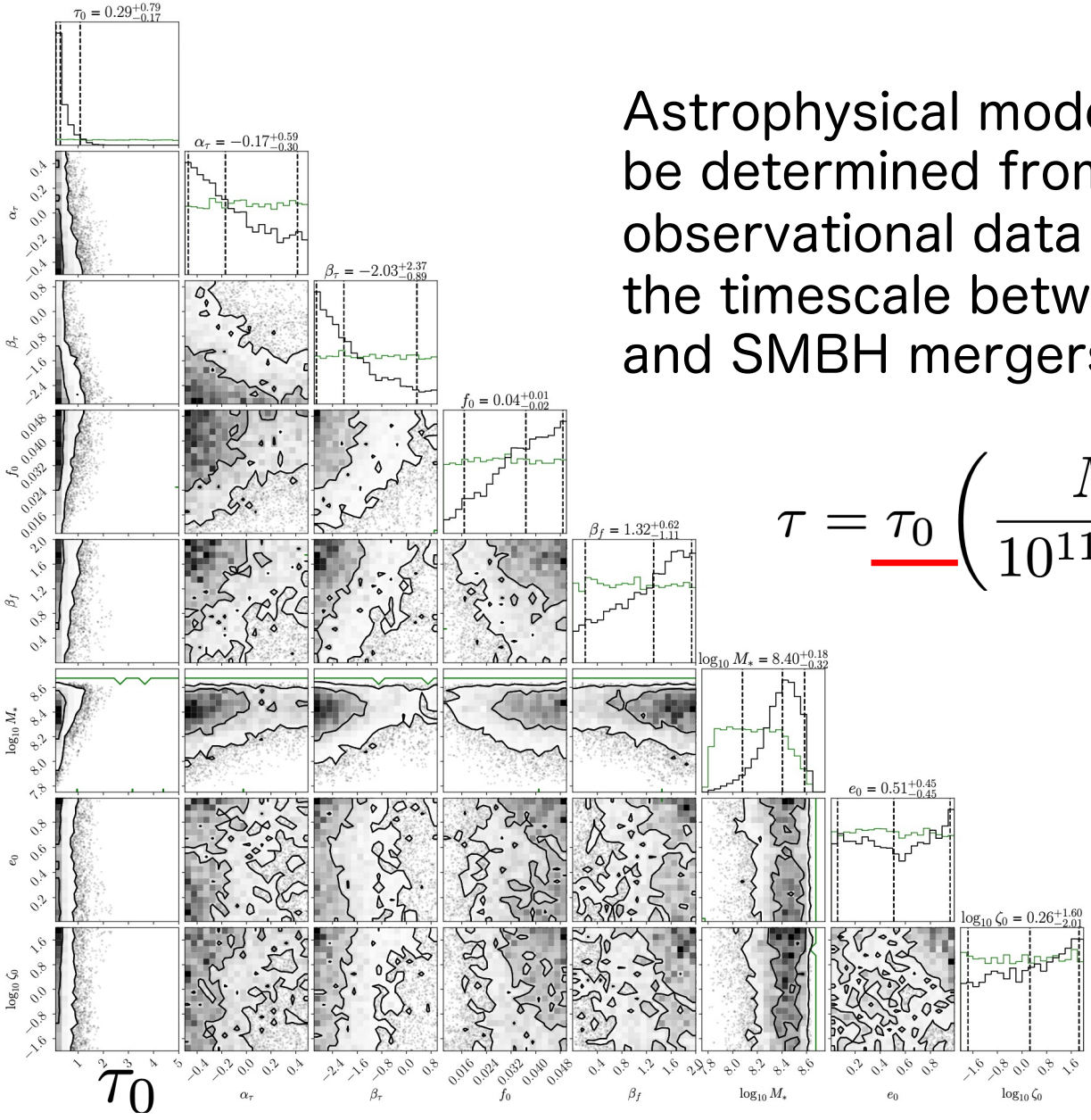

Astrophysical model parameters cannot be determined from the current observational data except for the timescale between galaxy mergers and SMBH mergers.

$$\tau = \tau_0 \left(\frac{M}{10^{11}\, M_\odot} \right)^{\alpha_\tau} (1+z)^{\beta_\tau} q^{\gamma_\tau}$$

Model comparison

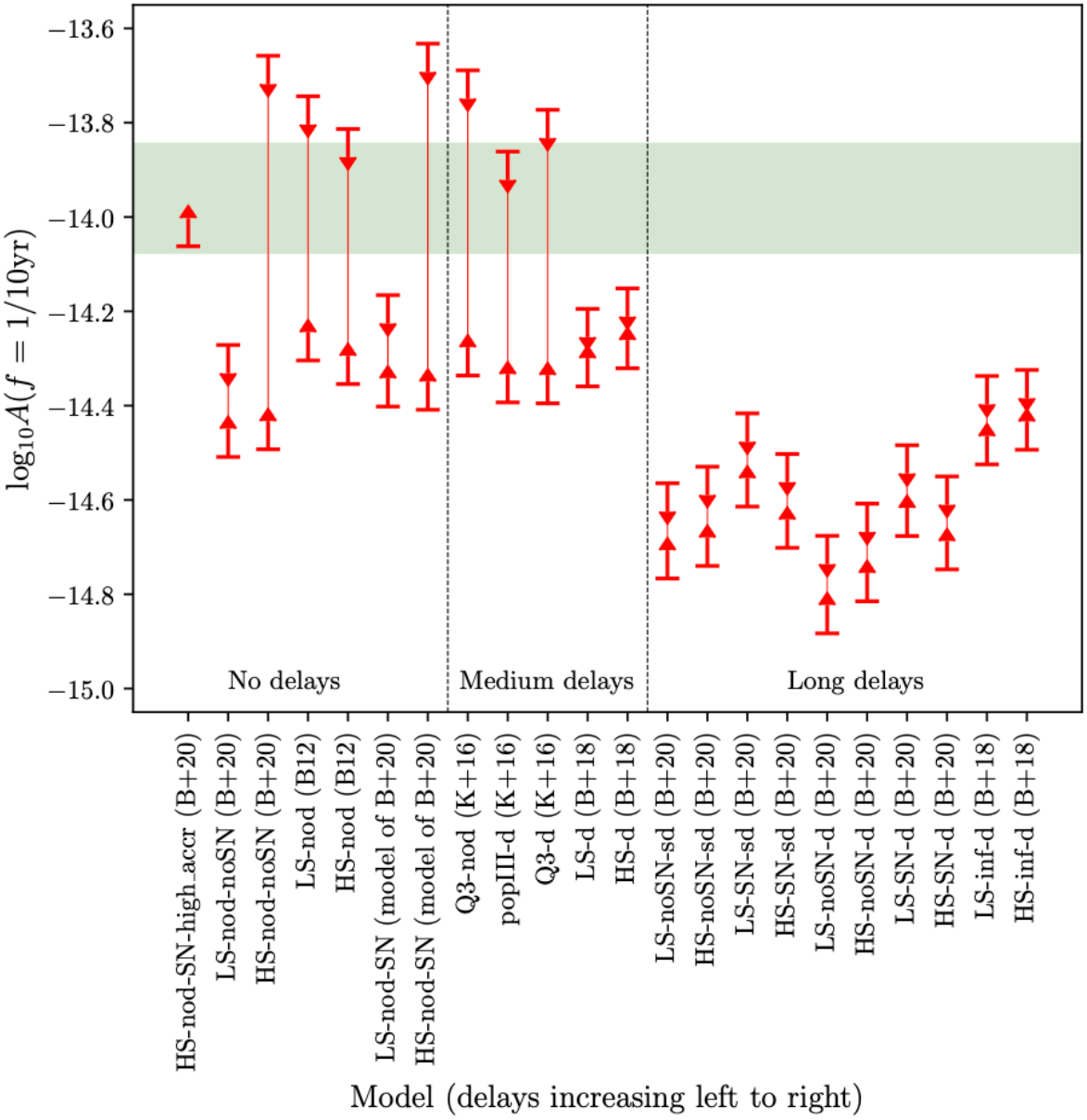

HS/popIII: high-mass seed
LS/Q3: low-mass seed

SN: supernova feedback on BH accretion

d: longer time delay
nod: no time delay

Shorter time delays are preferred.

Best models compatible with the data

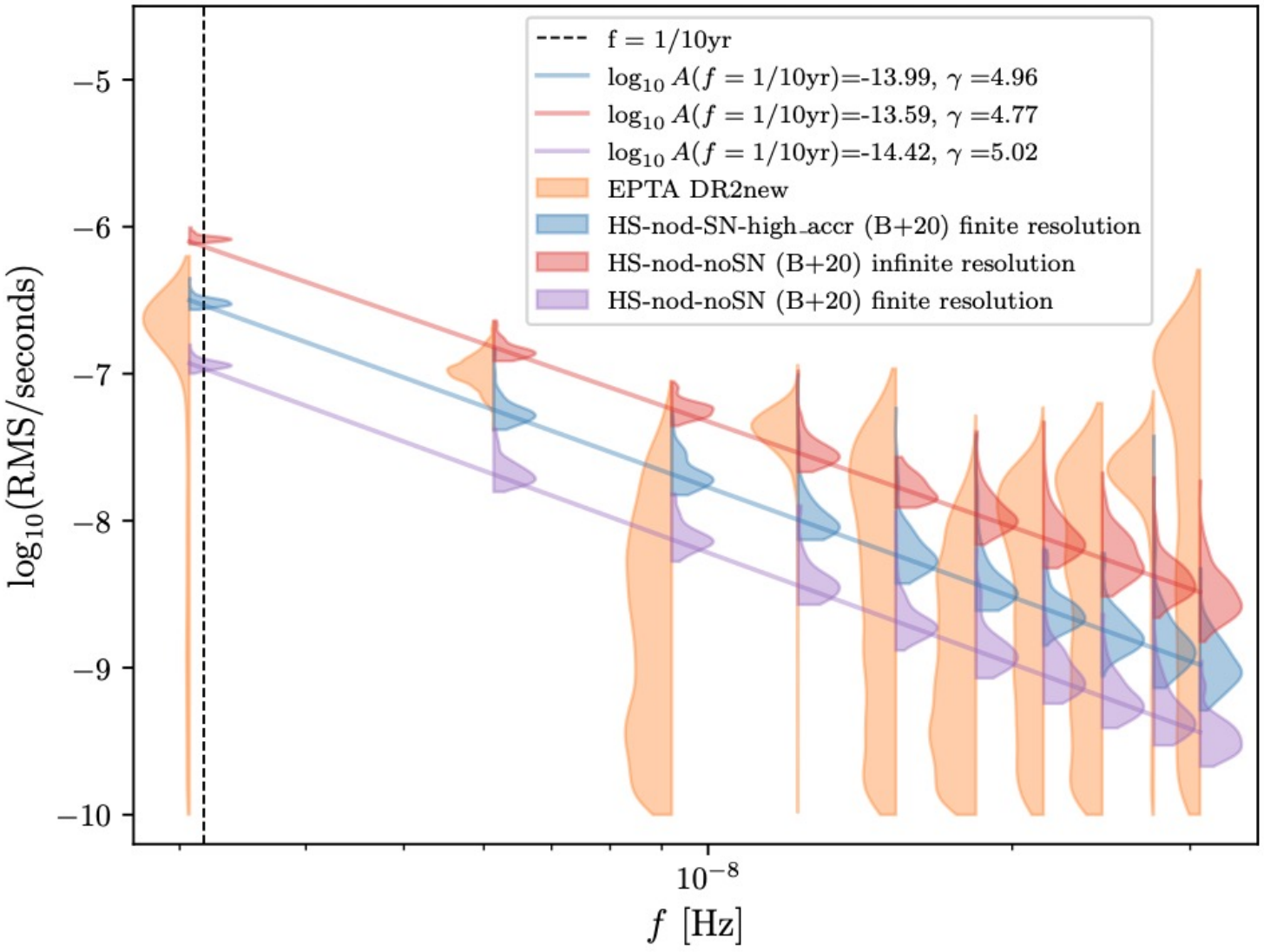

Anisotropic search

Agazie+ (NANOGrav), ApJL (2023)

For an anisotropic GWB, a correlation signal of time residuals

$$R_{ab}(t) = \frac{1}{3\sqrt{4\pi}} \int_{-\infty}^{\infty} \mathrm{d}f \, \frac{1-\cos(2\pi f t)}{(2\pi f)^2} I(f) \sum_{\ell m} c^I_{\ell m} \Gamma^I_{\ell m}(\xi_{ab}, f)$$

angular power spectrum $C_\ell = \frac{1}{2\ell+1} \sum_{m=-\ell}^{\ell} |c_{\ell m}|^2$

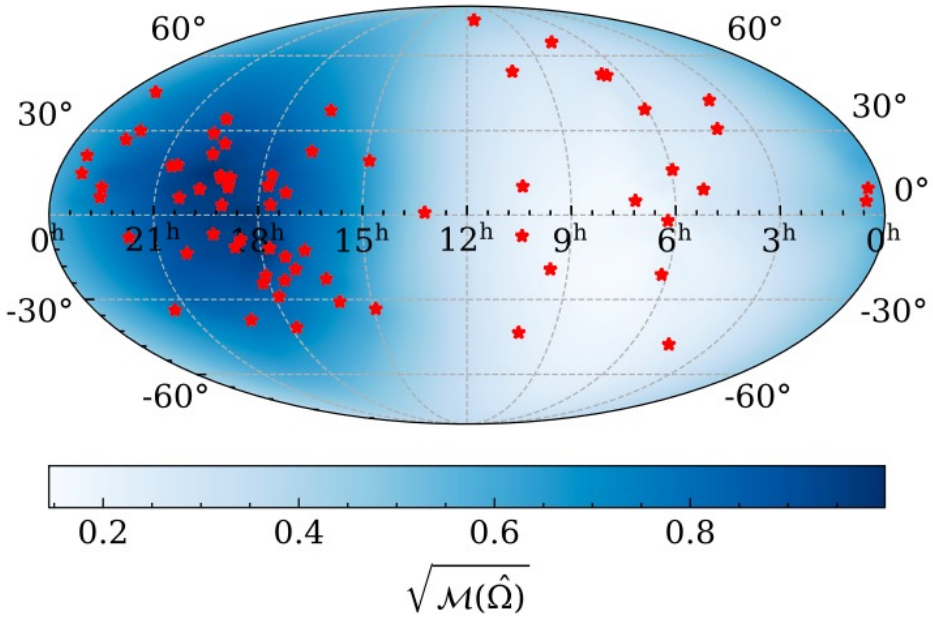

directional relative sensitivity

Anisotropic search results

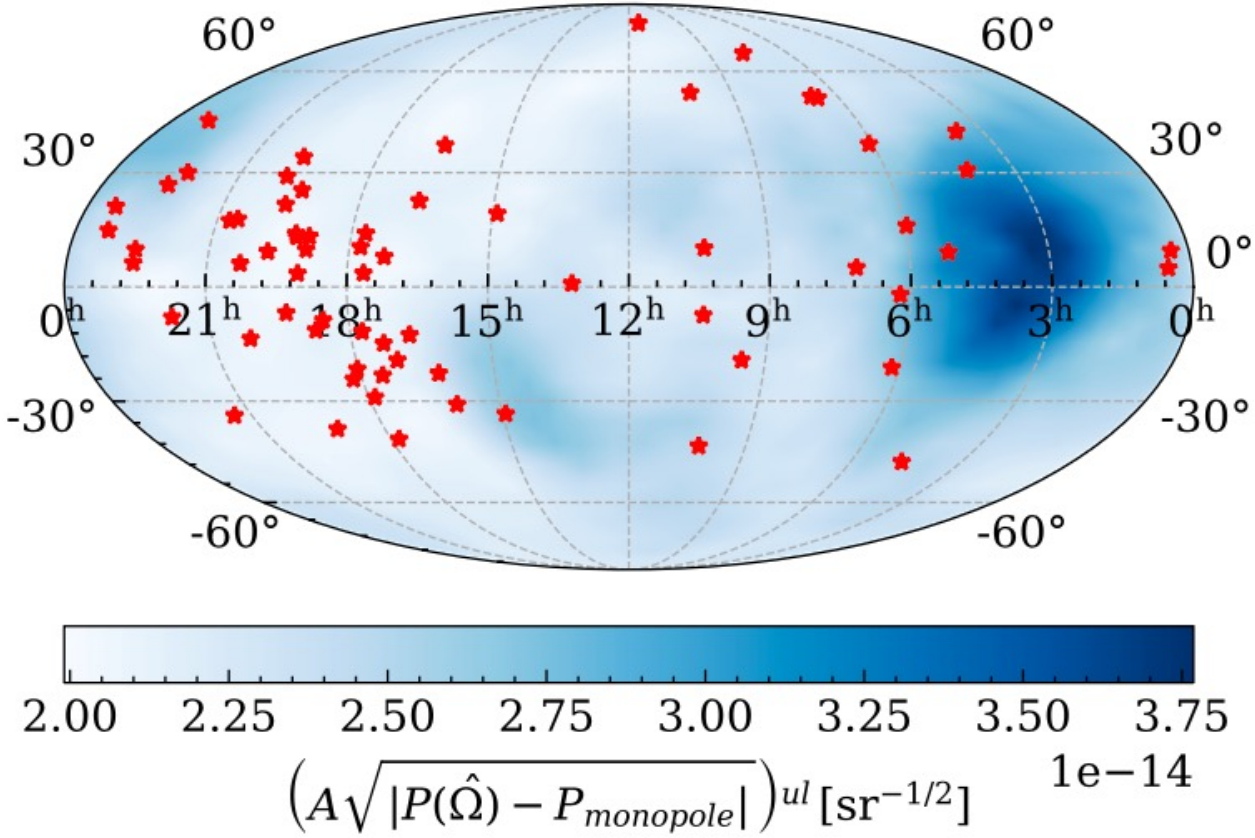

Slight excess power was found in the right region.

Anisotropic search results

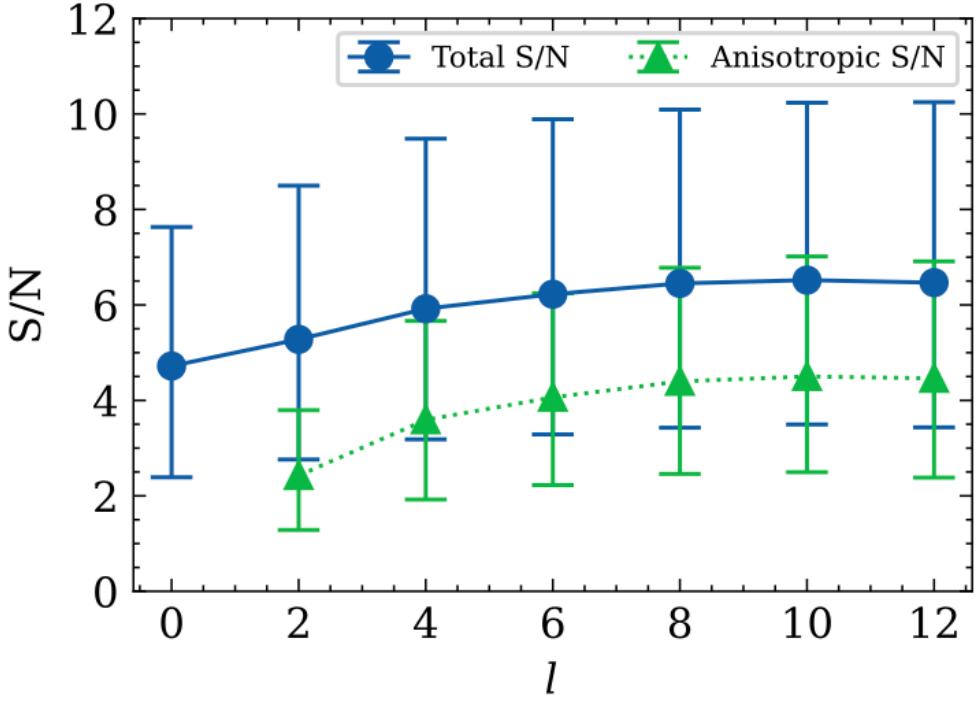

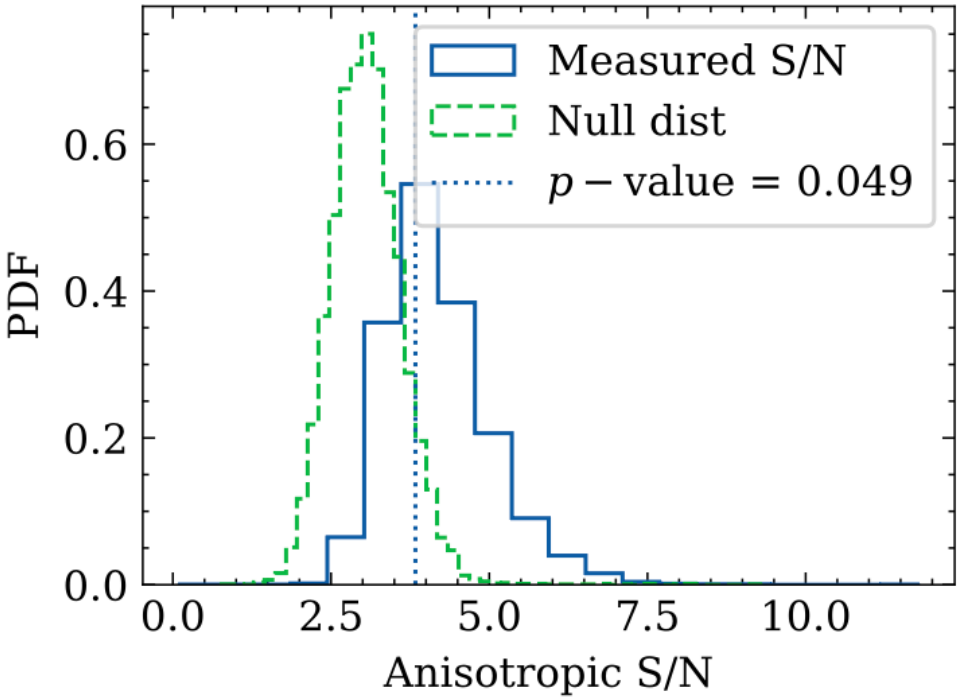

SNR for the multipoles are NOT significant.

No anisotropy was found. Consistent with an isotropic GWB.

Circular polarization from a binary

e.g. Valbusa Dall'Armi+, PRL (2023)

$$Q_\alpha(\iota) \equiv \begin{cases} \left(\frac{1+\cos^2\iota}{2}\right)^2 + \cos^2\iota & \alpha = I \\ (1+\cos^2\iota)\cos\iota & \alpha = V \end{cases}$$

$$p(\iota) = \frac{\sin\iota}{2} \quad \text{(isotropic dist.)}$$

$$\bar{\Omega}^I_{\rm AGWB} \sim \int d\iota\, p(\iota) Q_I(\iota) = \frac{4}{5}$$

$$\bar{\Omega}^V_{\rm AGWB} \sim \int d\iota\, p(\iota) Q_V(\iota) = 0$$

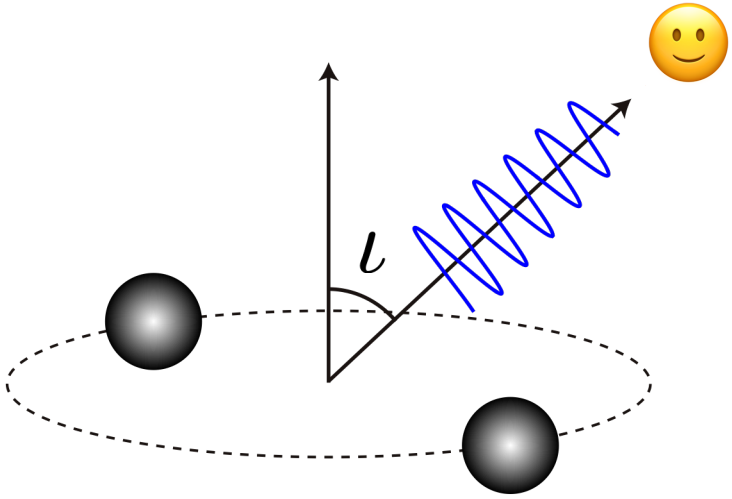

Circular pol. vanishes when integrated over the sky.

Number of sources in the pulsar timing band

Ellis+, A&A (2023)

Cumulative number of SMBHs heavier than $M_{\rm min}$

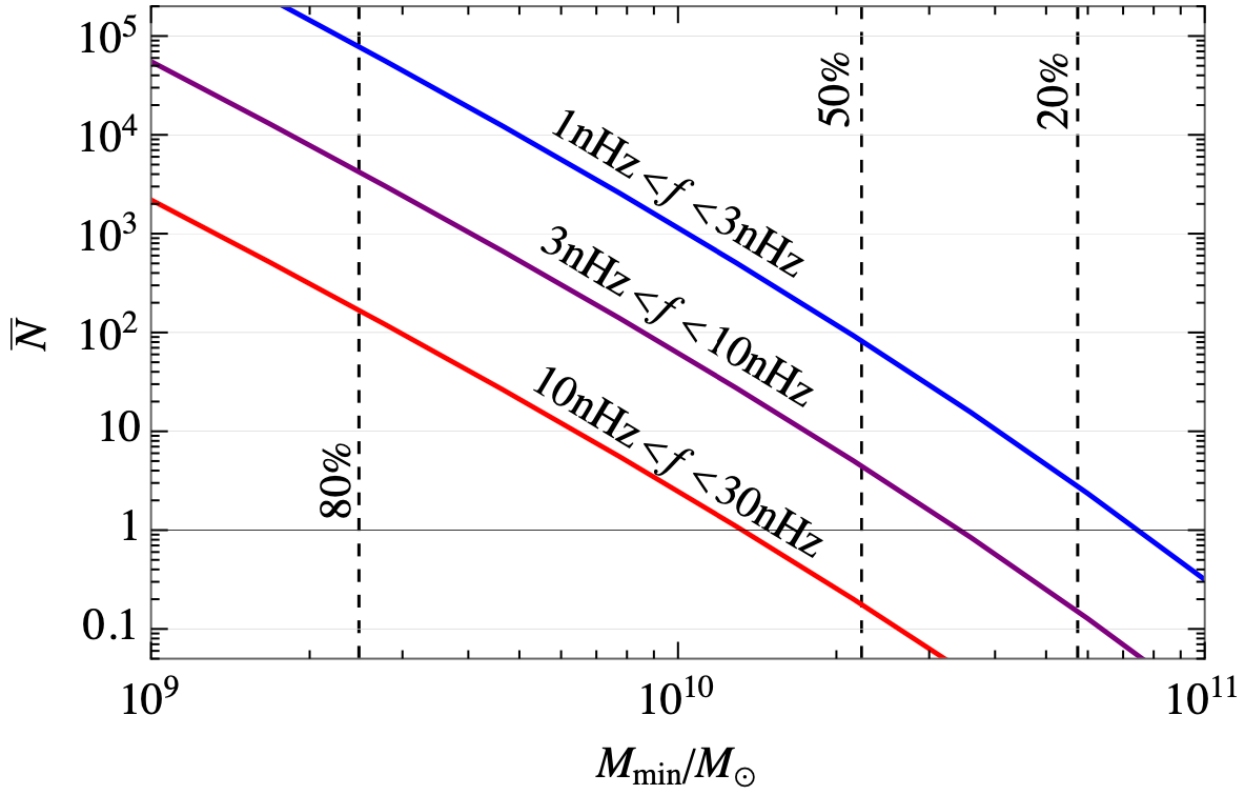

More sources in the pulsar-timing sensitive band and less at higher frequencies.

Circular polarization of GWB

Ellis+, A&A (2023)

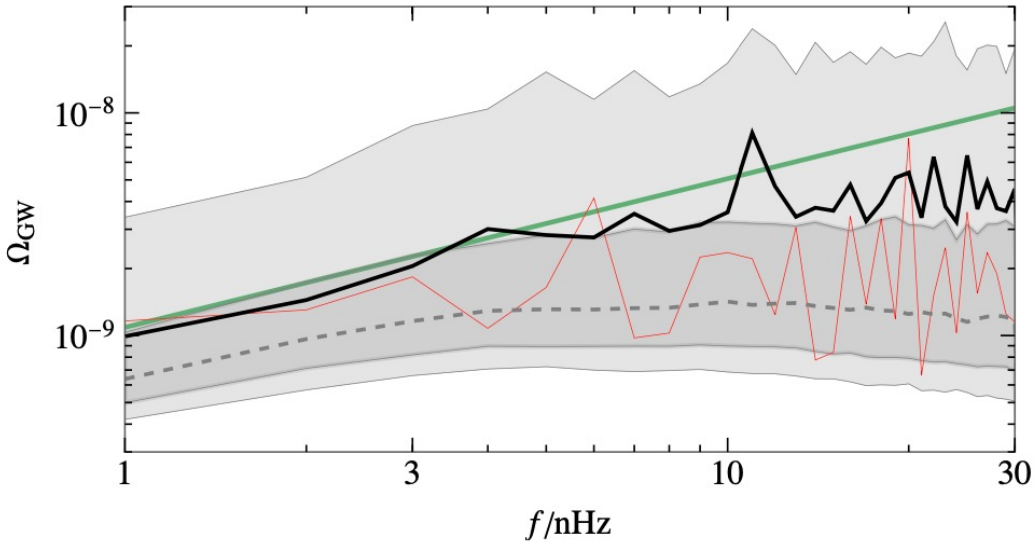

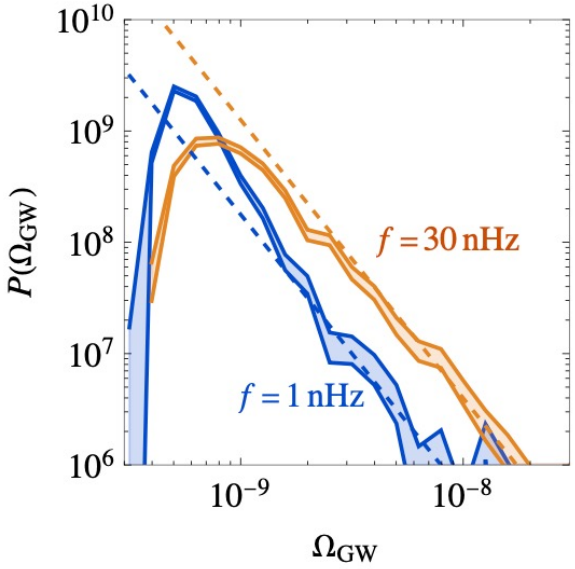

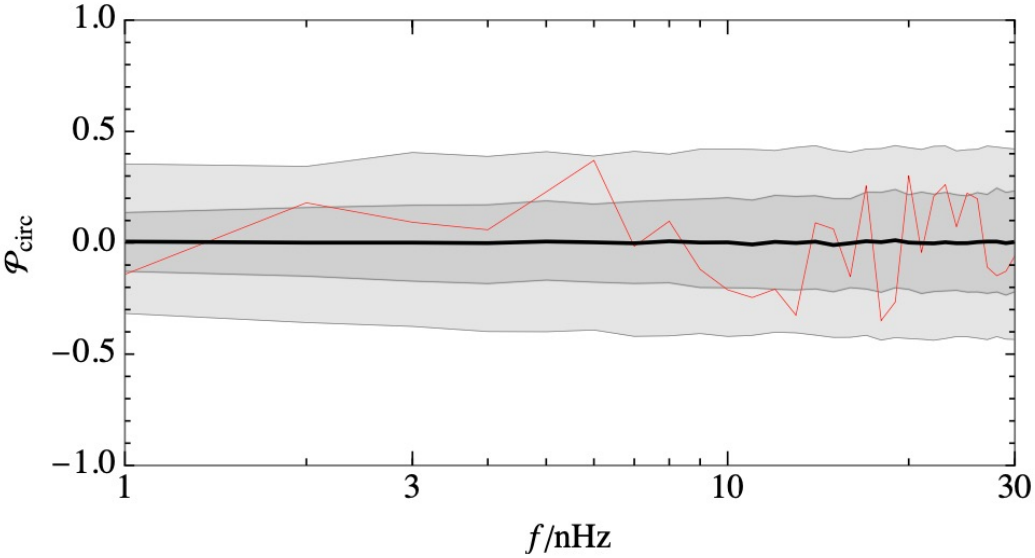

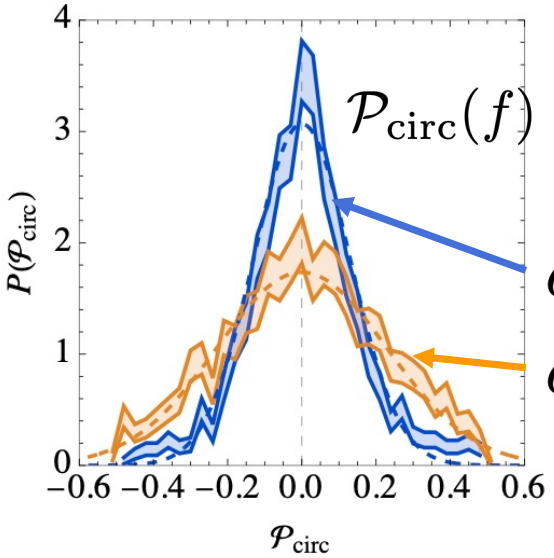

$$\mathcal{P}_{\rm circ}(f) = \frac{\sum_i V_i(f)}{\sum_i I_i(f)}$$

$\sigma = 0.13$

$\sigma = 0.23$

Summary of Part 2

- GW evidence: The Helling-Downs correlation has been detected with 2-4 σ significance.
- The signal is consistent with a GWB from SMBH binaries, but the origin is not identified yet.
- For a SMBH binary with $\mathcal{M}_{\rm c} \geq 10^7\, M_\odot$, the pulsar timing band is GW-driven (Binaries can merger in the cosmic time).
- For $\bar{R} \gtrsim 0.07\,{\rm pc}$, SMBH binaries need an efficient mechanism to push them to the pulsar timing band (subparsec problem).
- The observational data prefers the upper edge of the astrophysical prior on the amplitude or the merger rate.
- The astrophysical population parameters are not determined yet and the anisotropy has not been detected yet.